https://doi.org/10.5194/egusphere-2026-5330
Preprint. Discussion started: 11 September 2026


# High rates of N and C mineralization in upper permafrost of a thawing palsa mire and their implications for GHG dynamics

Richard E. Lamprecht[1], Kateřina Diáková[2], Carolina Voigt[1, 3, 4], Henri M. P. Siljanen[1], Hana Šantrůčková[2], Pertti J. Martikainen[1], Christina Biasi[1, 5], Maija E. Marushchak[1]

[1] University of Eastern Finland, Department of Environmental and Biological Sciences, Kuopio, Finland

[2] University of South Bohemia, Department of Ecosystem Biology, České Budějovice, Czech Republic

[3] University of Hamburg, Institute of Soil Science, Hamburg, Germany

[4] Permafrost Research Section, Alfred Wegener Institute Helmholtz Center for Polar and Marine Research, Potsdam, Germany

[5] University of Innsbruck, Institute of Ecology, Innsbruck, Austria

*Correspondence to*: Richard E. Lamprecht (richla@uef.fi)

Keywords: Arctic, palsa peat, incubation experiment, C mineralization, net N mineralization, nitrous oxide, temperature sensitivity, $Q_{10}$

https://doi.org/10.5194/egusphere-2026-5330
Preprint. Discussion started: 11 September 2026


**Abstract**

Rapid warming accelerates permafrost thaw in Arctic peatlands, exposing their large stocks of soil organic matter (SOM) to microbial decomposition. Despite the importance of permafrost peatlands for ecosystem-climate feedback, their coupled C and N mineralization potential and associated greenhouse gas (GHG) dynamics still remain poorly understood. Particularly interesting in this context is the upper permafrost, which is expected to thaw in near future and has been linked to substantial $CO_2$ and $N_2O$ production in previous studies.

Here, we investigated depth patterns of SOM mineralization and GHG production in a subarctic palsa mire in a factorial incubation experiment, where peat from active layer and upper permafrost was exposed to three temperatures (4, 10, and 16 °C) and two oxygen conditions (aerobic, anaerobic).

The highest rate of $CO_2$ production with the lowest temperature sensitivity were found in the surface peat and upper permafrost. Surface peat showed $CH_4$ consumption under aerobic condition, while $CH_4$ production was negligible across all peat depths and oxygen conditions. The highest rate and lowest temperature sensitivity of net N mineralization were found in upper permafrost and active layer-permafrost interface, but this did not translate into high $N_2O$ production; instead, the maximum $N_2O$ production occurred under anaerobic condition in the lower active layer.

Overall, our study revealed distinct depth patterns of C and N dynamics in palsa profiles, with high mineralization potential in the upper permafrost, supported by labile SOM. Relatively high mineralization rates at low temperatures resulted in low temperature sensitivity in the upper permafrost, and indicate high potential for C and N losses under realistic temperature range expected with gradual active layer deepening in the deep peat layers.

https://doi.org/10.5194/egusphere-2026-5330
Preprint. Discussion started: 11 September 2026


## 1 Introduction

Permafrost peatlands contain one of the largest terrestrial reservoirs for soil organic carbon (415±147 Pg C) and nitrogen (10±7 Pg N) and represent therefore a key component of the global permafrost-climate feedback (Hugelius et al., 2020; Schuur et al., 2015). With an area of $1.7\pm0.5 \times 10^6$ km$^2$, they comprise about half of the total northern peatland area (Hugelius et al., 2020). The large C and N stocks in permafrost peatlands have accumulated under cold and wet conditions, where decomposition is slow (Davidson and Janssens, 2006). With ongoing warming and permafrost thaw (Beilman and Robinson, 2003; Borge et al., 2017; Sannel et al., 2016; Swindles et al., 2015), decomposition processes in permafrost peatlands become less temperature limited, exposing their C and N stocks to microbial activities. While almost half of the permafrost peatland C stocks and most of the N stocks are currently in a frozen state within permafrost (Hugelius et al., 2020), gradual active layer deepening is widely documented (Streletskiy et al., 2026). Furthermore, the high ground ice content (Karjalainen et al., 2022) makes permafrost peatlands vulnerable for abrupt thaw, which causes rapid mobilization of C and N. Depending on thaw trajectory and environmental conditions prevailing after thaw, permafrost degradation may result in increased emissions of the greenhouse gases (GHGs) carbon dioxide ($CO_2$), methane ($CH_4$), and/or nitrous oxide ($N_2O$), thereby potentially creating a positive feedback to climate warming (Helbig et al., 2017; Schuur et al., 2008; Voigt et al., 2017a, b). However, predicting the magnitude and even direction of post-thaw GHG fluxes remains challenging, because warming and permafrost thaw alter various environmental factors simultaneously.

Temperature and moisture are primary controls of microbial decomposition and other microbial activities, together regulating GHG production and consumption rates in soil. While the response of C mineralization in permafrost peatlands to temperature and moisture has been extensively studied by incubation experiments (Baysinger et al., 2025; Diáková et al., 2016; Kjær et al., 2024; Schädel et al., 2016 and references therein), fewer studies have investigated N mineralization (Diáková et al., 2016; Keuper et al., 2012; Song et al., 2018) and $N_2O$ production (Song et al., 2022; Spiller et al., 2025). Incubation studies combining both C and N mineralization together with production of all three GHGs

https://doi.org/10.5194/egusphere-2026-5330
Preprint. Discussion started: 11 September 2026


are remarkably scarce (Song et al., 2022). Within the temperature range naturally occurring in northern soils, temperature generally enhances microbial activity including C and N mineralization (Liu et al., 2017; Schädel et al., 2014). However, temperature does not necessarily increase production of $N_2O$ or $CH_4$, since these gases represent the net balance of production and consumption processes, each of which is differentially regulated by temperature (Dunfield et al., 1993; Holtan-Hartwig et al., 2002). Furthermore, positive temperature effect is strongly modified by oxygen availability and the quantity and quality of C and N substrates.

Moisture content largely determines oxygen diffusion to the peat profile, thereby affecting the rate of C mineralization and the fraction of $CO_2$ and $CH_4$ in total C gas release Click or tap here to enter text.. Oxygen availability is also a key factor regulating mineral N transformation pathways which contribute to $N_2O$ production and consumption Click or tap here to enter text.. Well-drained conditions typically prevail in palsas and peat plateaus—ombrotrophic peat mounds in permafrost peatlands, uplifted above the surrounding mire surface by a permafrost core Click or tap here to enter text.. High oxygen availability in palsa peat enhances $CO_2$ production and N mineralization compared to permafrost-free wetlands with water-logged conditions Click or tap here to enter text.. Drier, oxygen-rich conditions also support other aerobic pathways such as $CH_4$ oxidation Click or tap here to enter text. and nitrification, as long as N substrate availability is not limiting Click or tap here to enter text.. Because of prevailing aerobic conditions, palsa surfaces typically do not show substantial $CH_4$ emissions *in-situ* but can act as sinks of atmospheric $CH_4$ Click or tap here to enter text.. A typical redox gradient from comparatively dry surface peat to water-saturated peat deeper in the profile supports $N_2O$ production via coupled nitrification-denitrification Click or tap here to enter text.. While gradual deepening of the active layer (i.e., seasonally thawing layer above permafrost) can initially promote aerobic pathways and overall decomposition rates by increasing the oxic soil volume, continued permafrost degradation or abrupt thaw leads to palsa collapse and initiation of water-logged conditions. Under wet anoxic conditions, decomposition is slower, and anaerobic microbial pathways, such as methanogenesis Click or tap here to enter text. and $N_2O$ reduction via denitrification can occur Click or tap here to enter text..

https://doi.org/10.5194/egusphere-2026-5330
Preprint. Discussion started: 11 September 2026


The availability of labile C and N compounds is another control on GHG production and consumption in permafrost peatlands (Pengerud et al., 2013). Susceptibility of SOM for mineralization, commonly referred to as SOM quality, differs greatly between and within peatlands but also according to the depth along the peat profile. Earlier studies have reported high biodegradability and content of dissolved organic carbon (DOC) (Fouché et al., 2020) and high mineral N content (Keuper et al., 2012; Wickland et al., 2018) in permafrost peat compared to the active layer. High contents of labile C and N substrates in permafrost layers are relevant for the permafrost-climate feedback because rapid C and N mineralization after permafrost thaw can promote emissions of $CO_2$, $CH_4$ and $N_2O$ (Knoblauch et al., 2018; Voigt et al., 2017a, 2019). Variability in SOM quality results mainly from two factors: I) the initial peat characteristics, determined by nutrient status and vegetation type during peat accumulation, II) the decomposition history, largely affected by permafrost aggradation-degradation history and the conditions before and after the frozen state (Jones et al., 2017; Treat et al., 2016). Further, downward leaching of water-soluble C and N compounds during the thaw season can contribute to the enrichment of labile C and N in the upper permafrost (Hansen and Elberling, 2023; Voigt et al., 2017a). High SOM quality affects not only the rate, but also the temperature sensitivity of mineralization: recalcitrant compounds are considered more sensitive to temperature increase than labile compounds (Conant et al., 2011; Fierer et al., 2005).

In this study, our aim was to assess the vulnerability of a permafrost peatland for C and N mineralization and associated GHG production, and investigate the dependence of these processes on temperature, oxygen availability and peat depth. For this purpose, we used sample material from an earlier permafrost thawing experiment, where we exposed intact peat mesocosms from a subarctic palsa mire to gradual thaw. When thawing reached upper permafrost in this previous mesocosm experiment, we observed enhanced $N_2O$ fluxes (Voigt et al., 2017a) and a larger contribution from deeper, old peat layers to surface $CO_2$ fluxes (Voigt et al., 2019), suggesting high lability of organic matter in this layer. We hypothesized that: I) C and N mineralization rates are higher in permafrost than in the active layer, but less sensitive to temperature increase, owing to the high content of labile organic matter in permafrost;

https://doi.org/10.5194/egusphere-2026-5330
Preprint. Discussion started: 11 September 2026


II) high mineralization rates in permafrost support high production of all three GHGs, $CO_2$, $CH_4$ and $N_2O$; III) C and N mineralization rates are significantly higher under aerobic than anaerobic conditions.

## 2 Materials and methods

### 2.1 Study site and soil sampling

In October 2012 peat cores were sampled at Peera Palsa Mire located near Kilpisjärvi, Finland (68° 89' N, 21° 05′ E) (Fig. 1a). The mean annual temperature in the region is –1.9 °C and the mean annual precipitation is 487 mm (1981-2010) (Pirinen et al., 2012). The sampling site is situated in the subarctic sporadic permafrost zone, also described as the palsa zone (Seppälä, 1988, 2006). The Peera Palsa is raised by frost heave up to ~3 m above the surrounding mire area. At the time of sampling, it showed signs of an early collapsing state (Kohout et al., 2014). Palsas in this area mainly developed between 3000 BP and 1000 BP (Oksanen, 2006; Seppälä, 1988, 2005). The palsa surface on Peera has typical ombrotrophic peatland vegetation including dwarf shrubs and herbaceous plants (e.g., *Betula nana* L., *Rubus chamaemorus*, *Empetrum nigrum*) and lichens (e.g., *Cladoniaceae*). Due to frost heave and wind abrasion, parts of the palsa surface are bare of vegetation(Seppälä, 2003).

The peat cores for this study were sampled from naturally bare peat surfaces on the top of the palsa (Fig. 1c, d), because high $N_2O$ emissions from such surfaces are well-documented by previous studies (Marushchak et al., 2011; Repo et al., 2009; Voigt et al., 2017b). A detailed description of the sampling site and procedure is given in the supplementary materials and methods section and in our previous publication by Voigt et al. (2017a). In brief: Four intact peat cores including the whole active layer plus 15 cm of the upper permafrost (total length of 71–92 cm) and a diameter of 10 cm were sampled using a custom-made coring device consisting of a stainless-steel corer with a replaceable polypropylene lining (Fig. S1a-c). Immediately after sampling, the peat cores were transferred within the plastic lining to a mild freezing temperature of –5 °C (±1 °C; SD) and stored for about five months before the

https://doi.org/10.5194/egusphere-2026-5330
Preprint. Discussion started: 11 September 2026


mesocosm thawing experiment. During the mesocosm experiment of 33-weeks, the peat cores were sequentially thawed from top to bottom, the native moisture content was contained by regular water additions, and fluxes of $CO_2$, $CH_4$, and $N_2O$ were continuously monitored (Voigt et al., 2017a, 2019). After the mesocosm experiment, the cores were refrozen to mild freezing temperatures and stored for six months before the start of the follow-up incubation experiment presented here.

### 2.2 Layer separation and preparation of peat for incubation experiment

Each intact peat core was divided into five sections. From the 15 cm of permafrost at the bottom of each core, we separated the lower 10 cm to the *permafrost table section (PFT)* and upper 5 cm with the bottom 5 cm of the active layer to the *permafrost–active layer interface section (PFI)* (Fig. 1b). The remaining active layer was divided into three equally heigh layers labelled from surface down as *active layer sections 1, 2 and 3 (AL1, AL2, and AL3)* (Fig. 1b). The active layer sections had different lengths (17–24 cm), depending on the total peat core length (Table S1). After cutting the cores sections in a frozen state (see supplementary information) (Fig. S2), they were thawed to +4°C (±2 °C) and homogenized by hand-mixing. Living roots, stones and big pieces of undecomposed wood were removed, if present.

### 2.3 Set-up of incubation experiment

The incubation experiment was carried out for 161 days (23 weeks) under aerobic and anaerobic conditions at three temperatures (4 °C, 10 °C, and 16 °C) (Fig. S3, S4; Table S3), following the incubation procedure described by Diáková et al. (2016). Prior to the start of the incubation experiment, we adjusted the water content of peat to 60% water holding capacity (WHC) for aerobic incubations and to 100% WHC for anaerobic incubations. After WHC adjustments, 30 g fresh weight (FW) subsamples of peat were weighed into air-tight 550 mL incubation flasks (Jouco Oy, Finland) which were closed with a rubber septum (Dätwyler, Switzerland) and tightened with aluminium crimp seals.

https://doi.org/10.5194/egusphere-2026-5330
Preprint. Discussion started: 11 September 2026


Aerobic incubation flasks contained ambient air as headspace gas and anaerobic flasks contained an oxygen-free, slightly over–pressured atmosphere consisting of 99 % dinitrogen ($N_2$) gas with 1 % carbon dioxide ($CO_2$). For each temperature and oxygen treatment set, we included one blank control (incubation flask without peat). More details are given in the supplementary materials and methods.

### 2.4 Gas sampling and analyses

The incubation flasks were kept closed during the incubation experiment for both aerobic and anaerobic treatments. The accumulation of $CO_2$, $CH_4$, $N_2O$ was measured weekly for the first five weeks and bi-weekly for the residual 18 weeks. The gas concentrations were measured at the start and end of each sampling interval (in total 13 intervals) (Fig. S4), and the difference between these concentrations was used to calculate the rate of gas production or consumption. In the start of each sampling interval, the incubation flasks were flushed with the headspace gas. The start gas samples (30 ml) were taken within 15 min from sealing the incubation flasks, and similar sampling took place in the end of each interval. 25 ml of the gas samples were transferred into 12 ml gas exetainers (Labco Exetainer ®, UK) for storage until concentration analysis. The sampled gas volume was compensated with air for aerobic flasks and with $N_2$ gas (5.0, AGA Industrial Gases, Finland) for anaerobic flasks. To avoid introducing $O_2$ into anaerobic flask, additional 30 ml of $N_2$ gas (5.0) was added to the headspace to establish a slight overpressure. Concentrations of $CO_2$, $CH_4$, $N_2O$ in the gas samples were analysed with a gas chromatograph (7890B GC System, Agilent Technologies, USA) coupled with an auto sampler (GX-271 Liquid Handler, Gilson, USA) as described in (Voigt et al., 2017a, 2019). Gas production rates were calculated per kg dry weight (DW) based on the ideal gas law and the concentration change between the start and end of each sampling interval. Cumulative GHG fluxes were calculated by summing up the fluxes for the whole incubation period of 161 days. Minor negative $CO_2$ and $CH_4$ fluxes under anaerobic conditions, which were occasionally observed during the incubation period, were considered negligible and set to zero for the calculation of the cumulative gas production. Although

https://doi.org/10.5194/egusphere-2026-5330
Preprint. Discussion started: 11 September 2026


possibility of chemoautotrophic $CO_2$ consumption or anaerobic $CH_4$ oxidation cannot be ruled out (Sabrekov et al., 2024), our incubation system was not designed for studying these processes.

### 2.5 Physical and chemical peat characteristics

Dry weight (DW), fresh bulk density (BD), water holding capacity (WHC), pH, and extractable mineral N content (ammonium ($NH_4^+$) and nitrate ($NO_3^-$)) were determined on fresh peat before the incubation experiment. Further physical and chemical analyses, including soil organic matter (SOM) content, total organic carbon (C) and nitrogen (N) content, and water-filled pore space (WFPS) were carried out on oven-dried peat (+60 °C, 48 h) using standard methods. More details of the peat analyses can be found in the supplementary materials and methods.

### 2.6 DOC, DON, microbial biomass carbon and aromaticity of DOC

Before the incubation, we determined the dissolved organic carbon (DOC) and total dissolved nitrogen (TDN) contents from 0.5 M $K_2SO_4$ extracts (1:4 w/v) with a TOC/TN analyser (LiquicTOC II, Elementar, Germany). Dissolved organic nitrogen (DON) was calculated by subtracting inorganic nitrogen as ammonium ($NH_4^+$) and nitrate ($NO_3^-$) from TDN.

Microbial biomass carbon ($C_{mic}$) was determined using the chloroform fumigation extraction method (Vance et al., 1987). The content of $C_{mic}$ was calculated as the difference in extractable C (0.5 M $K_2SO_4$, 1:4 w/v) between the fumigated and non-fumigated sub-samples. The yield of the fumigation extraction method was corrected for incomplete extraction of microbial carbon using factor $K_{EC} = 0.38$ (Vance et al., 1987).

The aromaticity of DOC as a proxy for DOC recalcitrance was determined from filtrated (0.45 µm) peat water extracts (ratio 1:2 v/v) based on the specific ultraviolet absorbance at a wavelength 254 nm ($SUVA_{254}$), which was normalized with the DOC concentration determined with a TOC/TN analyser

https://doi.org/10.5194/egusphere-2026-5330
Preprint. Discussion started: 11 September 2026


(Multi N/C 2100S, Analytic Jena AG, Germany). The aromaticity as % from DOC was calculated following (Weishaar et al., 2003).

### 2.7 Net nitrogen mineralization and nitrification

Net nitrogen mineralization ($N_{min}$) during aerobic and anaerobic incubation was calculated over the whole incubation period (161 days) as the difference of the initial and end content of extractable inorganic nitrogen ($NH_4^+ + NO_3^-$), divided by the time. For aerobic incubations, we further calculated the net nitrification ($N_{nit}$).

### 2.8 Temperature sensitivity of $CO_2$ production and net nitrogen mineralization

To assess the temperature sensitivity of aerobic and anaerobic respiration and net nitrogen mineralization, we calculated the temperature dependency coefficient $Q_{10}$ for each process and peat layer. The $Q_{10}$ is a commonly used index, representing the change in the rate ratio of a biological reaction with a temperature increase of 10 °C (Hamdi et al., 2013; Kirschbaum, 1995; Liu et al., 2017; Moni et al., 2015; Mundim et al., 2020). We did not calculate the $Q_{10}$ for $CH_4$ production due to mostly negligible production rates. The temperature sensitivity of $CO_2$ production ($Q_{10}CO_2$) was calculated by fitting to an exponential function to the cumulative $CO_2$ production rates over the full incubation period as a function of temperature using Equation 1, where $T$ is the incubation temperature and $R$ and $\alpha$ are fitted parameters (Fierer et al., 2005; Hamdi et al., 2013). The $Q_{10}CO_2$ was then calculated using the parameter $\alpha$ in equation 2.

$$CO_2\ production = R\, e^{\alpha T} \quad (1)$$

$$Q_{10}CO_2 = e^{10\alpha} \quad (2)$$

https://doi.org/10.5194/egusphere-2026-5330
Preprint. Discussion started: 11 September 2026


The temperature sensitivity of net nitrogen mineralization ($Q_{10}N_{min}$) was derived from the net nitrogen mineralization rates according to equation 3 (Liu et al., 2017). In the equation, $N_1$ and $N_2$ represent net nitrogen mineralization rates at given incubation temperatures, here 10 °C and 16 °C.

$$Q_{10}N_{min} = (N_2/N_1)\, e^{[10/(T_2-T_1)]} \quad (3)$$

### 2.9 Data processing and statistical analyses

Data processing, statistical analyses and graphical representation were performed using the R software (R version 4.5.1) (R Core Team, 2025). All graphics were prepared using *ggplot2* (Wickham, 2016). Data normality was visually inspected by histograms, density and Q-Q plots and tested using Shapiro-Wilk test. For non-normally distributed data, we performed $\log_{10}$ transformation, and used non-parametric tests if normality was not achieved.

Pairwise differences between peat layers were tested using one-way ANOVA with Tukey's HSD post hoc test (parametric test) or Kruskal-Wallis test with Dunn's test (non-parametric test) (*FSA*; (Ogle et al., 2025). This included peat characteristics, GHG production, net N mineralization rates within each temperature, as well as $Q_{10}CO_2$ and $Q_{10}N_{min}$. The peat layers were grouped based on significant differences ($P \leq 0.05$) using *agricolae* (de Mendiburu, 2020) or *rcompanion* (Mangiafico, 2020). Similar testing was used for differences between incubation temperatures within each peat layer.

Further, we tested differences between peat layers and incubation temperatures in cumulative GHG production, net N mineralization ($N_{min}$), net nitrification ($N_{nitr}$) the $Q_{10}CO_2$ and $Q_{10}N_{min}$ with linear mixed effect models using *lme4* (Bates et al., 2015). The modelling was done I) for all data combined including both aerobic and anaerobic conditions (temperature, peat depth and oxygen condition as fixed factors and the core number as random factor; Table 2), and 2) separately for each oxygen conditions (temperature and peat depth as fixed factors and the core number as random factor; Table 3, 4). The *P*-

https://doi.org/10.5194/egusphere-2026-5330
Preprint. Discussion started: 11 September 2026


values for model coefficients were obtained via Kenward–Roger approximations for the degrees of freedom with R package lmerTest (Kuznetsova et al., 2017).

The statistical significance of changes of DOC, DN, DON, $NH_4^+$ and $NO_3^-$ content during the incubation and differences between peat layers were evaluated separately for aerobic and anaerobic incubation conditions with linear mixed-effects models as described above (Tables S11–13).

The depth-specific differences in GHG production, $N_{min}$, $Q_{10}$ and peat characteristics and associations of these variables with each other were analyzed with principal component analyses (PCA) and Pearson's correlation analyses. The principal component analyses (PCA) were visualized using *factoextra* (Kassambara and Mundt, 2020) and the correlations using *ggcorrplot* (Kassambara, 2023).

## 3 Results

### 3.1 Physical and chemical peat characteristics

Many of the peat characteristics, determined before the incubation experiment, varied distinctly across the peat profile (ANOVA; Table 1). Active layer peat was significantly drier ($F(4, 15) = 8.30$, $P < 0.001$) compared to permafrost peat, while the permafrost interface had an intermediate moisture content. A similar increasing depth pattern was seen in DOC concentrations with significant differences between layers ($F(4, 15) = 3.76$, $P = 0.026$), and in DN and DON, although without significant differences. Aromaticity of DOC showed an opposite depth pattern, with the highest aromaticity in surface peat and the lowest in permafrost ($F(4, 15) = 7.69$, $P = 0.001$). The total C and N contents and C:N ratio did not show significant depth-dependent differences; instead, the variability of C:N ratio among replicate cores was high. While $NH_4^+$ content tended to increase with depth, and elevated $NO_3^-$ content was found in the top peat and permafrost, these depth patterns were not statistically significant due to high variability among replicates. Overall, $NH_4^+$ clearly dominated over $NO_3^-$ across the peat profile, with a 1–2 orders of magnitude higher content.

https://doi.org/10.5194/egusphere-2026-5330
Preprint. Discussion started: 11 September 2026


Additionally, we tested the changes of DOC, $C_{mic}$, DN, DON, $NH_4^+$, $NO_3^-$ and pH between the start and end of the incubation with linear mixed effects models (Fig. S7–S10; Tables S11–13). Under aerobic conditions, we found significant net accumulation of $NH_4^+$, especially in the permafrost layer (Fig. S9a). In the same treatment, $NO_3^-$ accumulated throughout the peat profile at 10 °C but only in the active layer at 16 °C, while it was completely consumed at 4 °C at all depths (Fig. S9b). DOC or DN did not change during aerobic conditions while $C_{mic}$, DON and pH significantly decreased (Fig. S7, 8 and 10). Under anaerobic conditions, we found significant increases during the incubation in DOC and $NH_4^+$ contents while DON content decreased (Fig. S7, 8, 9; Table S12). No significant changes were found in Cmic, DN, $NO_3^-$ and pH during the anaerobic incubation.

### 3.2 $CO_2$ production

Carbon dioxide production showed a positive temperature dependency under both oxygen treatments (Fig. 2; linear mixed effect model, $P < 0.001$; Table 3). We found higher rates under aerobic than anaerobic conditions (linear mixed effect model; $P < 0.001$; Fig. 2, Table 3), and this difference between oxygen treatments increased with temperature from 2.5-fold at 4 °C to 6-fold at 16 °C (Fig. 2, Table S9). Accordingly, the temperature sensitivity of $CO_2$ production ($Q_{10}CO_2$) was significantly higher under aerobic than anaerobic conditions (4.0±1.0 vs. 1.9±0.8, respectively; linear mixed effect model, $P < 0.001$). The depth pattern of $CO_2$ production was roughly similar under both oxygen treatments, with the highest rates in the top active layer and permafrost, and the lowest rates at variable depths in the active layer and permafrost interface (linear mixed effect model: aerobic: $P < 0.001$; anaerobic: $P <$ 0.001–0.003; Table 3). The depth pattern of $Q_{10}CO_2$ was opposite to the depth pattern of $CO_2$ production rate under both oxygen treatments, meaning that high $CO_2$ production rates were generally associated with low temperature sensitivities. The $Q_{10}CO_2$ under aerobic conditions decreased almost linearly with depth from 5.0±0.9 in the top active layer to 2.9±0.9 in permafrost. Under anaerobic conditions, the lowest $Q_{10}CO_2$ was similarly found in permafrost (1.2±0.5), but the highest in the mid profile (2.7±1.0) (Fig. 4).

https://doi.org/10.5194/egusphere-2026-5330
Preprint. Discussion started: 11 September 2026


### 3.3 $CH_4$ flux

The $CH_4$ flux during the incubation varied between significant net consumption to small net production (Fig. 2c, d; Table S4). Under aerobic conditions, we found net $CH_4$ consumption in the top active layer at all three incubation temperatures, resulting in a considerable, although statistically only marginally significant difference between oxygen treatments (linear mixed effect model, $P = 0.053$; Table 2). We did not observe any positive temperature dependency of $CH_4$ consumption (Table 3). Surprisingly, we observed small but persistent net production of $CH_4$ in permafrost interface and permafrost in aerobic conditions, but not in anaerobic conditions, where $CH_4$ production was negligible to marginal throughout the 23-week-long incubation throughout the peat profile (Fig. 2c, d; Table 3, Table S5).

### 3.4 Net N mineralization

We found 2 to 4-fold higher net N mineralization ($N_{min}$) under aerobic than anaerobic conditions (linear mixed effect model, $P < 0.001$; Table 2) (Fig. 3c, d, Table S7). The depth pattern of $N_{min}$ was similar under both oxygen treatments with uniform rates across the active layer, followed by an increase towards the permafrost layer (linear mixed effect model; $P < 0.001$ for both treatments; Table 4). A significant positive temperature dependency of $N_{min}$ was found in both oxygen treatments (linear mixed effect model; aerobic, 16 °C vs. 4 °C: $P = 0.002$; anaerobic, both 10 and 16 °C vs. 4 °C: $P < 0.001$; Table 4). The temperature sensitivity of $N_{min}$ ($Q_{10}N_{min}$) was similar in both oxygen treatments with overall means of 2.1±1.3 under aerobic and 2.0±1.4 under anaerobic conditions (linear mixed effect model, $P = 0.682$; Table 2) (Fig. 4, Table S9). The $Q_{10}N_{min}$ value decreased with peat depth under both oxygen conditions (linear mixed effect model; aerobic: $P < 0.001$–$0.004$; anaerobic: $P < 0.001$–$0.002$; Table 4).

Net nitrification rates ($N_{nit}$) in aerobic incubations were highly variable among replicates, resulting in ranges overlapping with zero and lack of significant differences between layers in most of the cases

https://doi.org/10.5194/egusphere-2026-5330
Preprint. Discussion started: 11 September 2026


(Fig. S6). A linear mixed effect model revealed a significantly higher $N_{nit}$ at 10 °C than at 4 °C ($P$ = 0.001; Table 4).

### 3.5 $N_2O$ production

During the 161-day incubation, we found higher $N_2O$ production under anaerobic than aerobic conditions (linear mixed effect model, $P$ = 0.017; Table 2) (Fig. 3a, b; Table S4, S6). Aerobic $N_2O$ production was negligible throughout the peat profile, while anaerobic $N_2O$ production peaked in the mid (AL2) and deep active layer (AL3), although the differences between layers were not statistically significant due to high variability among replicates (Fig. 3b, Table 4). Under anaerobic conditions, we observed a clear, negative temperature dependency of $N_2O$ production with the highest production rates at 4 °C, intermediate at 10 °C and lowest at 16 °C (Fig. 3b; Table S6; linear mixed effect model, $P$ = 0.011; Table 4). A clear temporal pattern was observed in anaerobic $N_2O$ production, which peaked in the beginning of the incubation at all temperatures, followed by net $N_2O$ consumption as the incubation progressed, especially at 16 °C (data not shown). The maximum rates during the early incubation were substantially (1-2 orders of magnitude) higher than the mean rates over the whole duration (Fig. S5).

### 3.6 Abiotic controls of C and N mineralization and GHG production

A principal component analysis (PCA) revealed distinct differences in peat characteristics, C and N mineralization rates, and greenhouse gas production between peat layers. More specifically, we found ordination of peat layers according to depth along the first principal component (PC1), with active layer and permafrost peat at the extreme ends of this axis (Fig. 5). Overall, the PCA results were largely similar in all three incubation temperatures, and the ordination was driven by the same variables, with only slight differences in variable contributions. The PCA of 4 °C data showed the clearest depth

https://doi.org/10.5194/egusphere-2026-5330
Preprint. Discussion started: 11 September 2026


separation, suggesting that the differences in the process rates were most pronounced at low temperatures (Fig. 5, Table S10).

The PC1 explained 36.8% of the overall variability in the data (Fig. 5). The main contributors to PC1 were $N_{min}$, $NH_4^+$, DN, DON, DOC, aromaticity of DOC, $CO_2$, $Q_{10}CO_2$, and WFPS (Fig. S11a). While the negative loadings of $NH_4^+$, $N_{min}$, WFPS, DOC, DN and DON indicate that these were higher in the permafrost than in the active layer, the opposite was true for $Q_{10}CO_2$, $Q_{10}N_{min}$, and aromaticity of DOC (Fig. 4; Table 1, S9). The second dimension (PC2) was mainly related to spatial differences between biological replicates. PC2 explained an additional 15.8% of variability (Fig. 5). The variables with strongest positive contributions to PC2 were C:N, $NO_3^-$, aerobic $Q_{10}CO_2$ and anaerobic $Q_{10}N_{min}$, while the total N content, $C_{mic}$ and aerobic $N_{nit}$ had negative contributions (Fig. S11b).

The results of the Pearson's correlation analysis were in a good agreement with the PCA findings (Fig. 6). We found strong positive correlations between $CO_2$ production and DOC content ($r = 0.6$, $p < 0.05$), Fig. 6), and between net N mineralization ($N_{min}$) and DOC, DN, DON, and $NH_4^+$ ($r = 0.5$–$0.9$, $p < 0.05$; Fig. 6). Statistically significant negative correlations were found between aerobic $Q_{10}CO_2$ and $N_{min}$ ($r =$ –0.5 to –0.6, $p < 0.05$; Fig. 6), as well as between aromaticity of DOC and $N_{min}$ ($r = –0.7$, $p < 0.05$; Fig. 6).

## 4 Discussion

### 4.1 Labile organic matter in permafrost supports high C and N mineralization rates

Our incubation study on peat cores from a subarctic palsa mire revealed distinct depth-related variability in C and N mineralization and GHG production. Our first hypothesis about high bioavailability of C and N in the permafrost layer, but low temperature sensitivity, was confirmed: We found high mineralization rates in the upper permafrost, similar (in the case of C) or higher (in the case of N) than the rates observed in the surface peat (Fig. 2, 3). The soil chemical analysis confirmed the highly

https://doi.org/10.5194/egusphere-2026-5330
Preprint. Discussion started: 11 September 2026


available C and N pool in the upper permafrost. Contents of extractable C (DOC) and N (DN, DON, $NH_4^+$) species were elevated in the deeper part of the profile and drove the separation between the peat layers in the PCA. As a further confirmation, the extractable C and N pools correlated positively with both $CO_2$ production and net N mineralization ($N_{min}$) rates irrespective of the oxygen treatment (Fig. 6).

Our findings of high N mineralization rates and elevated mineral N content in permafrost as compared to the active layer corroborate previous findings from various permafrost sediments (Hansen and Elberling, 2023; Strauss et al., 2022 and references therein). The accumulation of reactive N may result from downward leaching of soluble N to the permafrost table (Voigt et al., 2017b) and/or low C:N ratios at depth (Palmtag et al., 2022), supporting high N mineralization rates (Booth et al., 2005; Klemedtsson et al., 2005). In our case, the C:N ratio or the total N content did not show clear depth patterns, but the mean DON content in the beginning of the incubation was almost twice as high in the upper permafrost than other layers, suggesting a higher fraction of easily accessible organic N at depth (Table 1). This DON was supporting high N mineralization during the incubation, which resulted in a reduction of DON coupled with an increase of $NH_4^+$. Importantly, the high bioavailability of N in the upper permafrost layer points towards a fertilizer effect on plant productivity with permafrost thaw, potentially promoting C sequestration in a thawing palsa mire (Keuper et al., 2012). On the other hand, high supply of N from the upper permafrost will also support microbial decomposition, and thereby $CO_2$ emissions from deeper peat layers (Song et al., 2022; Wild et al., 2014). Predicting the net effect of these mechanisms, associated with opposite C fluxes, is a complex modelling task and beyond the scope of this study. However, our data can be used in such work for model validation purposes.

Due to negligible to marginal $CH_4$ production under both oxygen conditions in our study, $CO_2$ was almost the sole product of C mineralization. We observed the highest $CO_2$ production rates under both aerobic and anaerobic conditions in the surface peat but also at depth, in the active layer-permafrost interface and the upper permafrost (Fig. 2a, b; Tables S4, S5). A similar bimodal depth pattern of $CO_2$ production was previously observed in Norwegian palsa mires by Kjær et al. (2024), while other permafrost peatland studies have reported a decrease from the surface towards permafrost (Song et al.,

https://doi.org/10.5194/egusphere-2026-5330
Preprint. Discussion started: 11 September 2026


2014, 2026; Wang et al., 2013; Zuo et al., 2025), or no differences between active layer and permafrost (Treat et al., 2014). These differences in depth patterns between studies likely result from differences among peat types and decomposition stages. In our study, the depth pattern of the $CO_2$ production resembled the depth pattern of the DOC content (Table 1, Fig. 2a, b). The permafrost layer contained almost twice as much DOC than the active layer, and the permafrost DOC was more labile (as indicated by a lower $SUVA_{254}$ value). Accumulation of labile DOC at the permafrost table has been previously observed (Fouché et al., 2020) and, as discussed above for DON, can result from vertical leaching (Voigt et al., 2017b). The significant positive correlation of both aerobic and anaerobic $CO_2$ production with DOC confirms the importance of the water-soluble C pool for $CO_2$ production (Fig. 6).

The temperature sensitivities of C and N mineralization showed similar depth patterns, opposite to those of the process rates. For both processes, the $Q_{10}$ values declined progressively with depth, reaching the lowest values in the upper permafrost (Fig. 4). The negative correlations of $Q_{10}$ values with DOC content and positive correlations with DOC aromaticity suggest that the depth trends can be explained by differences in substrate quality (Fig. 6). Our findings align with the common theory of lower temperature sensitivity of C decomposition for labile than recalcitrant SOM (Conant et al., 2011; Fierer et al., 2005). According to a global meta-analysis, this theory applies also to N mineralization (Liu et al., 2017). The mean temperature sensitivities of ~4 and ~2 in our study for aerobic and anaerobic $CO_2$ production, respectively, compare well with the ranges reported in previous subarctic and boreal peatland studies (Diáková et al., 2016; Hamdi et al., 2013; Liu et al., 2024; Tarkhov et al., 2019). However, two synthesis studies have reported lower aerobic $Q_{10}$ values for peatlands (Schädel et al., 2016; Wang et al., 2019) which suggests that our peat was relatively recalcitrant. Similarly high temperature sensitivity of aerobic $CO_2$ production was previously observed on bare permafrost peatland surfaces (Diáková et al., 2016). The lower $Q_{10}$ values of both C and N mineralization in the upper permafrost than surface peat resulted from comparatively high rates already at low temperatures and a proportionally lower increase with warming. This has important implications for post-thaw mobilization of C and N. It suggests that microbes in permafrost peat are cold-adapted and, thus, active under the

https://doi.org/10.5194/egusphere-2026-5330
Preprint. Discussion started: 11 September 2026


low temperature range expected in the deep active layer after gradual thaw, enhancing the possibility for $CO_2$ losses and mineral N turnover.

### 4.2 Low $N_2O$ and $CH_4$ production in permafrost despite high mineralization rates

Contrary to our second hypothesis, high C and N mineralization rates in the upper permafrost did not translate into high rates of $CH_4$ or $N_2O$ production under either of the oxygen treatments. Despite the high mineral N content and net N mineralization rate, we did not find any $N_2O$ production in the upper permafrost or the permafrost interface; instead, the highest $N_2O$ production was observed in the middle to lower part of the active layer (Fig. 3b). This can be explained by initial differences in moisture content and their effects on the microbial assembly mediating N turnover. Before normalising the moisture for the incubations, the water-filled pore space (WFPS) in the permafrost layer was ~80% while it was only ~40–50% in the active layer (Table 1). The lower moisture content in the active layer favoured nitrifier activity, as indicated by our net nitrification data which peaked in the active layer, not permafrost (Fig. S6). Based on substantial $N_2O$ production only under anaerobic condition, denitrification was the dominant $N_2O$ production pathway in our study, similar to previous permafrost peatland studies (Gil et al., 2022; Palmer and Horn, 2012). However, the denitrifier $N_2O$ production is dependent on $NO_3^-$ and $NO_2^-$ supply from nitrification (Lamprecht et al., 2026). Other studies have shown that $N_2O$ production in permafrost can be limited by a low abundance of ammonia-oxidizers, responsible for the first step of nitrification (Marushchak et al., 2021; Monteux et al., 2020). It is possible that such microbial limitation was taking place also in our deeper peat layers; however, we are lacking direct microbial data to confirm this.

The high importance of coupled nitrification-denitrification process for $N_2O$ production in unfertilized soils poses a challenge for conventional soil incubation experiments, like ours, that target fully aerobic or anaerobic conditions. In our anaerobic incubation, we observed a temporary peak of $N_2O$ production, followed by net $N_2O$ consumption after the initial $NO_3^-$ was depleted and denitrifiers switched to using $N_2O$ as their electron acceptor. This may partially explain the lack of $N_2O$ production in the permafrost

https://doi.org/10.5194/egusphere-2026-5330
Preprint. Discussion started: 11 September 2026


451 layer: under the reductive conditions, the initial $NO_3^-$ was so quickly consumed that we did not capture
452 any $N_2O$ with our incubation set-up with weekly to biweekly sampling intervals. Similarly, the negative
453 temperature dependency of $N_2O$ production in our experiment can be explained by quicker consumption
454 of the initial $NO_3^-$ at higher temperatures than 4 °C.

455 An important question remains: what was causing the post-thaw increase in $N_2O$ emissions in the
456 preceding mesocosm experiment (Voigt et al., 2017a), if the upper permafrost did not produce any $N_2O$?
457 Increased $N_2O$ emissions following permafrost thaw may have resulted from a larger peat volume with
458 a favourable intermediate moisture content for coupled nitrification-denitrification, or from vertical
459 leaching of $NO_3^-$ produced in the upper, oxic peat layers to the deeper, anoxic layer, where it was
460 denitrified. These mechanisms could not be captured in our incubation experiment, where homogenized
461 peat from individual layers was incubated separately under either fully aerobic or fully anaerobic
462 conditions. Also, without microbial data on functional gene abundance and activity, the processes
463 underlying the increased $N_2O$ emissions in the mesocosms experiment remain partly inconclusive.
464 Despite this, our results demonstrate the added value of conducting parallel investigations using
465 mesocosm approaches and conventional soil incubations with discrete samples but also highlight the
466 importance of considering interactions between soil layers and gas transport processes.

467 In the oxic incubation, we found $CH_4$ consumption in the surface peat (Fig. 2c, Table 3, S4). This is
468 consistent with the net uptake of $CH_4$ we found in the preceding mesocosm experiment in the dry
469 scenario, imitating gradual active layer deepening (in contrast to a wet scenario, imitating palsa
470 collapse) (Voigt et al., 2019), as well as field measurements in palsa mires (Voigt et al., 2023).
471 Similarly, the lack of $CH_4$ production in our anaerobic treatment (Fig. 2d) is in accordance with the
472 negligible $CH_4$ emissions under the wet scenario of the mesocosm experiment (Voigt et al., 2019). The
473 lack of $CH_4$ production under the 5-month anaerobic incubation is likely a consequence of a very low
474 abundance or complete absence of active methanogens. In the uplifted palsa surfaces, the active layer
475 is well-aerated and rich with oxygenated compounds, such as $NO_3^-$ (Table 1), $SO_4^{2-}$, $Fe^{3+}$, and
476 oxygenated organic compounds, which can act as alternative electron acceptors and need to be reduced

https://doi.org/10.5194/egusphere-2026-5330
Preprint. Discussion started: 11 September 2026


before methanogenesis becomes favourable (Achtnich et al., 1995). This, together with the low initial abundance of methanogens, may prevent $CH_4$ production even under extended anoxia. In the upper permafrost, on the other hand, the long-term frozen conditions can cause limited microbial functionality due to lack of certain microbial groups or plant derived organics. For this reason, long lag-phases or complete absence of $CH_4$ production are commonly reported for oxic soil layers and permafrost soils (Knoblauch et al., 2018; Treat et al., 2016). Under anaerobic conditions, aerobic methanotrophs could also use produced $N_2O$ as source of oxygen as shown earlier (Awala et al., 2024; Hao et al., 2022), this could be a potential reason for limited $N_2O$ and $CH_4$ production under anoxic conditions. However, we do not have microbial data to support this theory. Interestingly, we found marginal $CH_4$ production rates in aerobic conditions in the deeper peat layers (Fig. 2c), similar to another subarctic peatland study (Diáková et al., 2016). This can be explained by $CH_4$ production in anaerobic microsites in trace amounts which could not be detected in the anaerobic treatment with $CH_4$-free headspace but were detectable in the aerobic treatment with ambient $CH_4$ concentration. Also, we cannot completely rule out the possibility for oxic $CH_4$ production (Knief, 2019).

### 4.3 Evidence for stronger warming impact under gradual than abrupt permafrost thaw

In confirmation of our third hypothesis, our results suggest different responses of C and N mineralization and GHG release from palsa mires to initial active layer deepening and continued or abrupt permafrost thaw. While both permafrost thaw trajectories will unlock the highly bioavailable C and N substrates in the upper permafrost, they will be differently affected by the contrasting hydrological and redox conditions. Active layer deepening will initially increase the oxic peat volume, whereas continued or abrupt permafrost thaw will result in palsa collapse and water saturated conditions. The higher overall GHG production in our study under aerobic than anaerobic conditions, strongly dominated by $CO_2$ production, suggests that gradual active layer deepening will result in higher GHG release. We found substantially higher $CO_2$ production under aerobic than anaerobic conditions, in accordance with the previous pan-arctic incubation synthesis (Schädel et al., 2016). Furthermore, the

https://doi.org/10.5194/egusphere-2026-5330
Preprint. Discussion started: 11 September 2026


response of $CO_2$ production to a temperature increase was stronger under aerobic than anaerobic conditions (Fig. 4, Table 2), a finding which has also been reported from other peatlands (Liu et al., 2024; Szafranek-Nakonieczna and Stêpniewska, 2014). The higher temperature sensitivity suggests stronger diurnal and seasonal dynamics under dry oxic conditions. Also, N mineralization rates was remarkably higher under aerobic than anaerobic conditions, suggesting higher reactive N supply with gradual active layer deepening compared to abrupt thaw (Fig. 3c, d). In this context it must be noted, however, that while gradual active layer deepening will expose the upper permafrost with high content of labile C for microbial decomposition, the peat will likely remain wet and poorly oxygenated in comparison to the surface peat, restricting the rate of decomposition compared to fully aerobic conditions in our aerobic treatment.

Under the different scenario that the palsa collapses, the decomposition of peat and associated $CO_2$ production will slow down. On the other hand, highly productive vegetation usually establishes in thermokarst wetlands and produces labile carbon, which could cause increased $CO_2$ and $CH_4$ production (Heffernan et al., 2022; Hodgkins et al., 2014). It is important to note that our anaerobic incubation likely underestimated the $CH_4$ production due to the microbial limitation of methanogenesis, which will be alleviated quickly in the real environment after the palsa collapses and gets exposed to highly reduced conditions and microbial invasion from the surrounding wetland. The same is true for any soil incubations with discrete samples, limiting their value for predicting ecosystem-climate feedback (Knoblauch et al., 2018). At the same time, classical soil incubations produce depth-resolved data and allow soil characteristics and GHG production to be linked by soil layer. As such, they serve as a valuable complement for field observations and mesocosm studies.

## 5 Conclusion

Our study demonstrates that the upper permafrost of palsa peatlands contains highly bioavailable C and N, making it particularly vulnerable to microbial mineralization and greenhouse gas production

https://doi.org/10.5194/egusphere-2026-5330
Preprint. Discussion started: 11 September 2026


following permafrost thaw. In addition to elevated concentrations of labile dissolved carbon and nitrogen, the significantly lower aromaticity of dissolved organic matter provides independent evidence that the upper permafrost contains a less recalcitrant, more bioavailable carbon and nitrogen pools than the overlying active layer. Despite the relatively low temperature sensitivity, the high substrate availability in the upper permafrost resulted in the highest $CO_2$ production rates. This suggests that substrate availability rather than temperature sensitivity will dominate the initial $CO_2$ response to permafrost thaw, and that comparatively high $CO_2$ production can be expected in the lower part of peat profile despite cold conditions at depth. In contrast, $N_2O$ production was primarily controlled by oxygen availability and coupled oxic-anoxic transformations rather than substrate availability, indicating that future $N_2O$ emissions cannot be predicted from peat characteristics alone. These findings highlight, that reliable predictions of the permafrost–climate feedback require consideration of both, substrate quality and the spatial organization of redox conditions. It is important to consider the possibility of functional limitations due to absence of certain microbial groups in permafrost when designing experiments and interpreting data; however, in the real environment, such limitations are likely quickly removed.

https://doi.org/10.5194/egusphere-2026-5330
Preprint. Discussion started: 11 September 2026


## 6 Code availability

The R code for the data analyses is available upon request.

## 7 Data availability

The data of this study, analyzed and generated, is provided in full within the article and its supplementary information.

## 8 Supplementary information

The supplementary information text (Supplementary_Information.pdf) comprises of more detailed descriptions of the peat core sampling, the incubation experiment procedure and analyses performed. Furthermore, the supplementary information includes additional figures and tables supporting the text.

## 9 Author contribution

C.B., H.S., P.J.P., K.D. and R.E.L planned and designed the experiment. R.E.L., C.V. and M.E.M. sampled the peat cores in the field. R.E.L and K.D. performed the incubation experiment and relating chemical analyses, gas analyses and data calculations. R.E.L., with the support and supervision of C.V., H.M.P.S. and M.E.M., further processed data, performed statistical analyses and prepared the graphs. R.E.L., with supervision of H.M.P.S., C.B. and M.E.M. wrote the first draft of the manuscript. All authors have discussed and revised the manuscript.

https://doi.org/10.5194/egusphere-2026-5330
Preprint. Discussion started: 11 September 2026


## 10 Competing interests

The authors declare that they have no conflict of interest.

## 11 Acknowledgements

The authors are grateful for financial support from the Nordic Center of Excellence DEFROST. The authors thank the Kilpisjärvi Biological Station for accommodation and the support with necessary materials for the field measurements and peat sampling.

R.E.L. received personal funding from the UEF doctoral program in Environmental Physics, Health and Biology and from the Finnish Cultural Foundation (Suomen Kulttuurirahasto) (grant no. 00170598 and 00180628).

C.V. was supported by the project MOMENT (03F0931A) funded by the German Federal Ministry of Research, Technology and Space (BMFTR), the European Research Council Starting Grant COLDSPOT (no. 101163177), and by Schmidt Sciences (PeTCaT, G-25-69377).

C.B. wishes to thank the Academy of Finland (project N-PERM, decision no. 341348; project NOCA, decision no. 314630 and the Yedoma-N project, decision no. 287469) for financial support, as well as the PERNO project supported by FWF, Austria (grant no. M03335).

M.E.M. was funded by the Research Council of Finland in the frame Thaw-N (349503, 353858)

https://doi.org/10.5194/egusphere-2026-5330
Preprint. Discussion started: 11 September 2026


## 12 References

Achtnich, C., Bak, F., and Conrad, R.: Competition for electron donors among nitrate reducers, ferric iron reducers, sulfate reducers, and methanogens in anoxic paddy soil, Biol. Fertil. Soils, 19, 65–72, https://doi.org/10.1007/BF00336349/METRICS, 1995.

Awala, S. I., Gwak, J. H., Kim, Y., Jung, M. Y., Dunfield, P. F., Wagner, M., and Rhee, S. K.: Nitrous oxide respiration in acidophilic methanotrophs, Nat. Commun., 15, 4226-, https://doi.org/10.1038/s41467-024-48161-z, 2024.

Bates, D., Mächler, M., Bolker, B., and Walker, S.: Fitting Linear Mixed-Effects Models Using lme4, J. Stat. Softw., 67, 1–48, https://doi.org/10.18637/jss.v067.i01, 2015.

Baysinger, M. R., Laurent, M., Verdonen, M., Reif, J., Kumpula, T., Liebner, S., and Treat, C. C.: Abrupt Thaw in a Finnish Palsa: Potential CH4 Production Driven by Vegetation Adaptation in the Transition From Permafrost to Post-Thaw Soils, J. Geophys. Res. Biogeosci., 130, e2025JG008847, https://doi.org/10.1029/2025JG008847, 2025.

Beilman, D. W. and Robinson, S. D.: Peatland permafrost thaw and landform type along a climatic gradient, in: Proceedings of the 8th International Conference on Permafrost, 61–65, 2003.

Booth, M. S., Stark, J. M., and Rastetter, E.: CONTROLS ON NITROGEN CYCLING IN TERRESTRIAL ECOSYSTEMS: A SYNTHETIC ANALYSIS OF LITERATURE DATA, Ecol. Monogr., 75, 139–157, https://doi.org/10.1890/04-0988, 2005.

Borge, A. F., Westermann, S., Solheim, I., and Etzelmüller, B.: Strong degradation of palsas and peat plateaus in northern Norway during the last 60 years, Cryosphere, 11, 1–16, https://doi.org/10.5194/tc-11-1-2017, 2017.

https://doi.org/10.5194/egusphere-2026-5330
Preprint. Discussion started: 11 September 2026


598 Butterbach-Bahl, K., Philippot, L., Serra, J., Silver, W. L., Ogle, S., and Abalos, D.: Three Decades of
599 Soil N2O Research—Insights and Gaps, Glob. Chang. Biol., 32, e71038,
600 https://doi.org/10.1111/GCB.71038, 2026.

601 Conant, R. T., Ryan, M. G., Ågren, G. I., Birge, H. E., Davidson, E. A., Eliasson, P. E., Evans, S. E.,
602 Frey, S. D., Giardina, C. P., Hopkins, F. M., Hyvönen, R., Kirschbaum, M. U. F., Lavallee, J. M.,
603 Leifeld, J., Parton, W. J., Megan Steinweg, J., Wallenstein, M. D., Martin Wetterstedt, J. Å., and
604 Bradford, M. A.: Temperature and soil organic matter decomposition rates - synthesis of current
605 knowledge and a way forward, https://doi.org/10.1111/j.1365-2486.2011.02496.x, 1 November 2011.,
606 2011.

607 Davidson, E. A. and Janssens, I. A.: Temperature sensitivity of soil carbon decomposition and
608 feedbacks to climate change, Nature, 440, 165–173, https://doi.org/10.1038/nature04514, 2006.

609 Diáková, K., Čapek, P., Kohoutová, I., Mpamah, P. A., Bárta, J., Biasi, C., Martikainen, P. J., and
610 Šantrůčkova, H.: Heterogeneity of carbon loss and its temperature sensitivity in East-European
611 subarctic tundra soils, FEMS Microbiol. Ecol., 92, fiw140, https://doi.org/10.1093/femsec/fiw140,
612 2016.

613 Dunfield, P., knowles, R., Dumont, R., and Moore, T. R.: Methane production and consumption in
614 temperate and subarctic peat soils: Response to temperature and pH, Soil Biol. Biochem., 25, 321–326,
615 https://doi.org/10.1016/0038-0717(93)90130-4, 1993.

616 Fan, Z., Neff, J. C., Waldrop, M. P., Ballantyne, A. P., and Turetsky, M. R.: Transport of oxygen in soil
617 pore-water systems: implications for modeling emissions of carbon dioxide and methane from
618 peatlands, Biogeochemistry, 121, 455–470, https://doi.org/10.1007/S10533-014-0012-0/FIGURES/5,
619 2014.

620 Fierer, N., Craine, J. M., Mclauchlan, K., and Schimel, J. P.: Litter quality and the temperature
621 sensitivity of decomposition, Ecology, 86, 320–326, https://doi.org/10.1890/04-1254, 2005.

https://doi.org/10.5194/egusphere-2026-5330
Preprint. Discussion started: 11 September 2026


622 Fouché, J., Christiansen, C. T., Lafrenière, M. J., Grogan, P., and Lamoureux, S. F.: Canadian
623 permafrost stores large pools of ammonium and optically distinct dissolved organic matter, Nat.
624 Commun., 11, 1–11, https://doi.org/10.1038/s41467-020-18331-w, 2020.

625 Gil, J., Marushchak, M. E., Rütting, T., Baggs, E. M., Pérez, T., Novakovskiy, A., Trubnikova, T.,
626 Kaverin, D., Martikainen, P. J., and Biasi, C.: Sources of nitrous oxide and the fate of mineral nitrogen
627 in subarctic permafrost peat soils, Biogeosciences, 19, 2683–2698, https://doi.org/10.5194/bg-19-2683-
628 2022, 2022.

629 Hamdi, S., Moyano, F., Sall, S., Bernoux, M., and Chevallier, T.: Synthesis analysis of the temperature
630 sensitivity of soil respiration from laboratory studies in relation to incubation methods and soil
631 conditions, Soil Biol. Biochem., 58, 115–126, https://doi.org/10.1016/j.soilbio.2012.11.012, 2013.

632 Hansen, H. F. E. and Elberling, B.: Spatial Distribution of Bioavailable Inorganic Nitrogen From
633 Thawing Permafrost, Global Biogeochem. Cycles, 37, e2022GB007589,
634 https://doi.org/10.1029/2022GB007589, 2023.

635 Hao, Q., Wang, O., Jiao, J. Y., Xiao, L., Zhang, Y., Li, W. J., and Liu, F.: Methylobacter couples
636 methane oxidation and N2O production in hypoxic wetland soil, Soil Biol. Biochem., 175, 108863,
637 https://doi.org/10.1016/J.SOILBIO.2022.108863, 2022.

638 Heffernan, L., Cavaco, M. A., Bhatia, M. P., Estop-Aragonés, C., Knorr, K. H., and Olefeldt, D.: High
639 peatland methane emissions following permafrost thaw: enhanced acetoclastic methanogenesis during
640 early successional stages, Biogeosciences, 19, 3051–3071, https://doi.org/10.5194/BG-19-3051-2022,
641 2022.

642 Helbig, M., Chasmer, L. E., Desai, A. R., Kljun, N., Quinton, W. L., and Sonnentag, O.: Direct and
643 indirect climate change effects on carbon dioxide fluxes in a thawing boreal forest–wetland landscape,
644 Glob. Chang. Biol., 23, 3231–3248, https://doi.org/10.1111/gcb.13638, 2017.

645 Hodgkins, S. B., Tfaily, M. M., McCalley, C. K., Logan, T. A., Crill, P. M., Saleska, S. R., Rich, V. I.,
646 and Chanton, J. P.: Changes in peat chemistry associated with permafrost thaw increase greenhouse gas

https://doi.org/10.5194/egusphere-2026-5330
Preprint. Discussion started: 11 September 2026


production, Proceedings of the National Academy of Sciences, 111, 5819–5824, https://doi.org/10.1073/pnas.1314641111, 2014.

Holtan-Hartwig, L., Dörsch, P., and Bakken, L. R.: Low temperature control of soil denitrifying communities: kinetics of N2O production and reduction, Soil Biol. Biochem., 34, 1797–1806, https://doi.org/10.1016/S0038-0717(02)00169-4, 2002.

Hugelius, G., Loisel, J., Chadburn, S., Jackson, R. B., Jones, M., MacDonald, G., Marushchak, M., Olefeldt, D., Packalen, M., Siewert, M. B., Treat, C., Turetsky, M., Voigt, C., and Yu, Z.: Large stocks of peatland carbon and nitrogen are vulnerable to permafrost thaw, Proc. Natl. Acad. Sci. U. S. A., 117, 20438–20446, https://doi.org/10.1073/pnas.1916387117, 2020.

Jones, M. C., Harden, J., O'Donnell, J., Manies, K., Jorgenson, T., Treat, C., and Ewing, S.: Rapid carbon loss and slow recovery following permafrost thaw in boreal peatlands, Glob. Chang. Biol., 23, 1109–1127, https://doi.org/10.1111/gcb.13403, 2017.

Karjalainen, O., Aalto, J., Kanevskiy, M. Z., Luoto, M., and Hjort, J.: High-resolution predictions of ground ice content for the Northern Hemisphere permafrost region, Earth System Science Data Discussion [preprint], 1–40 pp., https://doi.org/10.5194/essd-2022-144, 2022.

Kassambara, A.: Visualization of a Correlation Matrix using "ggplot2" [R package ggcorrplot version 0.1.4.1], CRAN: Contributed Packages, https://doi.org/10.32614/CRAN.PACKAGE.GGCORRPLOT, 2023.

Kassambara, A. and Mundt, F.: factoextra: Extract and Visualize the Results of Multivariate Data Analyses, https://cran.r-project.org/package=factoextra, 2020., 2020.

Keuper, F., van Bodegom, P. M., Dorrepaal, E., Weedon, J. T., van Hal, J., van Logtestijn, R. S. P., and Aerts, R.: A frozen feast: Thawing permafrost increases plant-available nitrogen in subarctic peatlands, Glob. Chang. Biol., 18, 1998–2007, https://doi.org/10.1111/j.1365-2486.2012.02663.x, 2012.

https://doi.org/10.5194/egusphere-2026-5330
Preprint. Discussion started: 11 September 2026


670 Kirschbaum, M. U. F.: The temperature dependence of soil organic matter decomposition, and the effect
671 of global warming on soil organic C storage, Soil Biol. Biochem., 27, 753–760,
672 https://doi.org/10.1016/0038-0717(94)00242-S, 1995.

673 Kjær, S. T., Westermann, S., Nedkvitne, N., and Dörsch, P.: Carbon degradation and mobilisation
674 potentials of thawing permafrost peatlands in northern Norway inferred from laboratory incubations,
675 Biogeosciences, 21, 4723–4737, https://doi.org/10.5194/bg-21-4723-2024, 2024.

676 Klemedtsson, L., Von Arnold, K., Weslien, P., and Gundersen, P.: Soil CN ratio as a scalar parameter
677 to predict nitrous oxide emissions, Glob. Chang. Biol., 11, 1142–1147, https://doi.org/10.1111/J.1365-
678 2486.2005.00973.X, 2005.

679 Knief, C.: Diversity of methane-cycling microorganisms in soils and their relation to oxygen, Curr.
680 Issues Mol. Biol., 33, 23–56, https://doi.org/10.21775/CIMB.033.023, 2019.

681 Knoblauch, C., Beer, C., Liebner, S., Grigoriev, M. N., and Pfeiffer, E. M.: Methane production as key
682 to the greenhouse gas budget of thawing permafrost, Nat. Clim. Chang., 1–4,
683 https://doi.org/10.1038/s41558-018-0095-z, 2018.

684 Kohout, T., Bućko, M. S., Rasmus, K., Leppäranta, M., and Matero, I.: Non-Invasive Geophysical
685 Investigation and Thermodynamic Analysis of a Palsa in Lapland, Northwest Finland, Permafr.
686 Periglac. Process., 25, 45–52, https://doi.org/10.1002/ppp.1798, 2014.

687 Kuznetsova, A., Brockhoff, P. B., and Christensen, R. H. B.: lmerTest Package: Tests in Linear Mixed
688 Effects Models, J. Stat. Softw., 82, 1–26, https://doi.org/10.18637/jss.v082.i13, 2017.

689 Lamprecht, R. E., Marushchak, M. E., Voigt, C., Bagnoud, A., Alves, R. J. E., Schleper, C.,
690 Martikainen, P., Biasi, C., and Siljanen, H. M. P.: Response of ammonia-oxidizing archaea to
691 experimental warming in high-N2O-emitting permafrost peatland habitats, Arct. Sci.,
692 https://doi.org/10.1139/as-2025-0075, 2026.

https://doi.org/10.5194/egusphere-2026-5330
Preprint. Discussion started: 11 September 2026


693 Liu, H., Rezanezhad, F., Zhao, Y., He, H., Van Cappellen, P., and Lennartz, B.: The apparent
694 temperature sensitivity (Q10) of peat soil respiration: A synthesis study, Geoderma, 443, 116844,
695 https://doi.org/10.1016/j.geoderma.2024.116844, 2024.

696 Liu, Y., Wang, C., He, N., Wen, X., Gao, Y., Li, S., Niu, S., Butterbach-Bahl, K., Luo, Y., and Yu, G.:
697 A global synthesis of the rate and temperature sensitivity of soil nitrogen mineralization: latitudinal
698 patterns and mechanisms, Glob. Chang. Biol., 23, 455–464, https://doi.org/10.1111/gcb.13372, 2017.

699 Mangiafico, S.: rcompanion: Functions to Support Extension Education Program Evaluation,
700 https://cran.r-project.org/package=rcompanion, 2020., 2020.

701 Marushchak, M. E., Pitkämäki, A., Koponen, H., Biasi, C., Seppälä, M., and Martikainen, P. J.: Hot
702 spots for nitrous oxide emissions found in different types of permafrost peatlands, Glob. Chang. Biol.,
703 17, 2601–2614, https://doi.org/10.1111/j.1365-2486.2011.02442.x, 2011.

704 Marushchak, M. E., Kerttula, J., Diáková, K., Faguet, A., Gil, J., Grosse, G., Knoblauch, C.,
705 Lashchinskiy, N., Martikainen, P. J., Morgenstern, A., Nykamb, M., Ronkainen, J. G., Siljanen, H. M.
706 P., van Delden, L., Voigt, C., Zimov, N., Zimov, S., and Biasi, C.: Thawing Yedoma permafrost is a
707 neglected nitrous oxide source, Nature Communications 2021 12:1, 12, 1–10,
708 https://doi.org/10.1038/s41467-021-27386-2, 2021.

709 de Mendiburu, F.: agricolae: Statistical Procedures for Agricultural Research, https://cran.r-
710 project.org/package=agricolae%0A, 2020., 2020.

711 Moni, C., Lerch, T. Z., Knoth de Zarruk, K., Strand, L. T., Forte, C., Certini, G., and Rasse, D. P.:
712 Temperature response of soil organic matter mineralisation in arctic soil profiles, Soil Biol. Biochem.,
713 88, 236–246, https://doi.org/10.1016/j.soilbio.2015.05.024, 2015.

714 Monteux, S., Keuper, F., Fontaine, S., Gavazov, K., Hallin, S., Juhanson, J., Krab, E. J., Revaillot, S.,
715 Verbruggen, E., Walz, J., Weedon, J. T., and Dorrepaal, E.: Carbon and nitrogen cycling in Yedoma
716 permafrost controlled by microbial functional limitations, Nat. Geosci., 13, 794–798,
717 https://doi.org/10.1038/s41561-020-00662-4, 2020.

https://doi.org/10.5194/egusphere-2026-5330
Preprint. Discussion started: 11 September 2026


718 Mundim, K. C., Baraldi, S., Machado, H. G., and Vieira, F. M. C.: Temperature coefficient (Q10) and
719 its applications in biological systems: Beyond the Arrhenius theory, Ecol. Modell., 431, 109127,
720 https://doi.org/10.1016/j.ecolmodel.2020.109127, 2020.

721 Nykänen, H., Heikkinen, J. E. P., Pirinen, L., Tiilikainen, K., and Martikainen, P.: Annual CO2
722 exchange and CH4 fluxes on a subarctic palsa mire during climatically different years, Global
723 Biogeochem. Cycles, 17, 1018, https://doi.org/10.1029/2002GB001861, 2003.

724 Ogle, D. H., Doll, J. C., Wheeler, A. P., and Dinno, A.: FSA: Simple Fisheries Stock Assessment
725 Methods, https://fishr-core-team.github.io/FSA/, 2025., 2025.

726 Oksanen, P. O.: Holocene development of the Vaisjeäggi palsa mire, Finnish Lapland, Boreas, 35, 81–
727 95, https://doi.org/10.1111/j.1502-3885.2006.tb01114.x, 2006.

728 Palmer, K. and Horn, M. A.: Actinobacterial nitrate reducers and proteobacterial denitrifiers are
729 abundant in N2O-metabolizing palsa peat, Appl. Environ. Microbiol., 78, 5584–5596,
730 https://doi.org/10.1128/AEM.00810-12, 2012.

731 Palmtag, J., Obu, J., Kuhry, P., Richter, A., Siewert, M. B., Weiss, N., Westermann, S., and Hugelius,
732 G.: A high spatial resolution soil carbon and nitrogen dataset for the northern permafrost region based
733 on circumpolar land cover upscaling, Earth Syst. Sci. Data, 14, 4095–4110,
734 https://doi.org/10.5194/essd-14-4095-2022, 2022.

735 Pengerud, A., Cécillon, L., Johnsen, L. K., Rasse, D. P., and Strand, L. T.: Permafrost Distribution
736 Drives Soil Organic Matter Stability in a Subarctic Palsa Peatland, Ecosystems, 16, 934–947,
737 https://doi.org/10.1007/s10021-013-9652-5, 2013.

738 Pirinen, P., Simola, H., Aalto, J., Kaukoranta, J.-P., Karlsson, P., and Ruuhela, R.: Tilastoja suomen
739 ilmastosta 1981-2010, Raportteja, 96 pp., http://hdl.handle.net/10138/35880, 2012.

740 R Core Team: R: A Language and Environment for Statistical Computing, https://www.r-project.org/,
741 2025., 2025.

https://doi.org/10.5194/egusphere-2026-5330
Preprint. Discussion started: 11 September 2026


742 Repo, M. E., Susiluoto, S., Lind, S. E., Jokinen, S., Elsakov, V., Biasi, C., Virtanen, T., and Martikainen,
743 P. J.: Large N2O emissions from cryoturbated peat soil in tundra, Nat. Geosci., 2, 189–192,
744 https://doi.org/10.1038/ngeo434, 2009.

745 Sabrekov, A. F., Semenov, M. V., Terentieva, I. E., Krasnov, G. S., Kharitonov, S. L., Glagolev, M. V.,
746 and Litti, Y. V.: Anaerobic methane oxidation is quantitatively important in deeper peat layers of boreal
747 peatlands: Evidence from anaerobic incubations, in situ stable isotopes depth profiles, and microbial
748 communities, Science of the Total Environment, 916, 170213,
749 https://doi.org/10.1016/j.scitotenv.2024.170213, 2024.

750 Sannel, A. B. K., Hugelius, G., Jansson, P., and Kuhry, P.: Permafrost Warming in a Subarctic Peatland
751 – Which Meteorological Controls are Most Important?, Permafr. Periglac. Process., 27, 177–188,
752 https://doi.org/10.1002/ppp.1862, 2016.

753 Schädel, C., Schuur, E. A. G., Bracho, R., Elberling, B., Knoblauch, C., Lee, H., Luo, Y., Shaver, G.
754 R., and Turetsky, M. R.: Circumpolar assessment of permafrost C quality and its vulnerability over time
755 using long-term incubation data, Glob. Chang. Biol., 20, 641–652, https://doi.org/10.1111/gcb.12417,
756 2014.

757 Schädel, C., Bader, M. K. F., Schuur, E. A. G., Biasi, C., Bracho, R., Čapek, P., De Baets, S., Diáková,
758 K., Ernakovich, J., Estop-Aragones, C., Graham, D. E., Hartley, I. P., Iversen, C. M., Kane, E.,
759 Knoblauch, C., Lupascu, M., Martikainen, P. J., Natali, S. M., Norby, R. J., O'Donnell, J. A.,
760 Chowdhury, T. R., Šantrůčková, H., Shaver, G., Sloan, V. L., Treat, C. C., Turetsky, M. R., Waldrop,
761 M. P., and Wickland, K. P.: Potential carbon emissions dominated by carbon dioxide from thawed
762 permafrost soils, Nat. Clim. Chang., 6, 950–953, https://doi.org/10.1038/nclimate3054, 2016.

763 Schuur, E. A. G., Bockheim, J., Canadell, J. G., Euskirchen, E., Field, C. B., Goryachkin, S. V.,
764 Hagemann, S., Kuhry, P., Lafleur, P. M., Lee, H., Mazhitova, G., Nelson, F. E., Rinke, A., Romanovsky,
765 V. E., Shiklomanov, N., Tarnocai, C., Venevsky, S., Vogel, J. G., and Zimov, S. A.: Vulnerability of

https://doi.org/10.5194/egusphere-2026-5330
Preprint. Discussion started: 11 September 2026


permafrost carbon to climate change: Implications for the global carbon cycle, Bioscience, 58, 701–714, https://doi.org/10.1641/B580807, 2008.

Schuur, E. A. G., McGuire, A. D., Schädel, C., Grosse, G., Harden, J. W., Hayes, D. J., Hugelius, G., Koven, C. D., Kuhry, P., Lawrence, D. M., Natali, S. M., Olefeldt, D., Romanovsky, V. E., Schaefer, K., Turetsky, M. R., Treat, C. C., and Vonk, J. E.: Climate change and the permafrost carbon feedback, Nature, 520, 171–179, https://doi.org/10.1038/nature14338, 2015.

Seppälä, M.: Palsas and related forms, in: Advances in Periglacial Geomorphology, edited by: Clark, M. J., John Wiley & Sons, Ltd, 247–278, 1988.

Seppälä, M.: Surface abrasion of palsas by wind action in Finnish Lapland, Geomorphology, 52, 141–148, https://doi.org/10.1016/S0169-555X(02)00254-4, 2003.

Seppälä, M.: Dating of palsas, Special Paper of the Geological Survey of Finland, 79–84, 2005.

Seppälä, M.: Palsa mires in Finland, The Finnish Environment, 23, 155–162, 2006.

Seppälä, M.: Synthesis of studies of palsa formation underlining the importance of local environmental and physical characteristics, Quat. Res., 75, 366–370, https://doi.org/10.1016/j.yqres.2010.09.007, 2011.

Siljanen, H. M. P., Alves, R. J. E., Ronkainen Jussi, G., Lamprecht, R. E., Bhattarai, H. R., Bagnoud, A., Marushchak, M. E., Martikainen, P. J., Schleper, C., and Biasi, C.: Archaeal nitrification is a key driver of high nitrous oxide emissions from arctic peatlands, Soil Biol. Biochem., 107539, https://doi.org/10.1016/j.soilbio.2019.107539, 2019.

Song, C., Wang, X., Miao, Y., Wang, J., Mao, R., and Song, Y.: Effects of permafrost thaw on carbon emissions under aerobic and anaerobic environments in the Great Hing'an Mountains, China, Science of the Total Environment, 487, 604–610, https://doi.org/10.1016/j.scitotenv.2013.09.083, 2014.

https://doi.org/10.5194/egusphere-2026-5330
Preprint. Discussion started: 11 September 2026


788 Song, Y., Song, C., Hou, A., Ren, J., Wang, X., Cui, Q., and Wang, M.: Effects of temperature and root
789 additions on soil carbon and nitrogen mineralization in a predominantly permafrost peatland, Catena
790 (Amst)., 165, 381–389, https://doi.org/10.1016/J.CATENA.2018.02.026, 2018.

791 Song, Y., Cheng, X., Song, C., Li, M., Gao, S., Liu, Z., Gao, J., and Wang, X.: Soil CO2 and N2O
792 emissions and microbial abundances altered by temperature rise and nitrogen addition in active-layer
793 soils of permafrost peatland, Front. Microbiol., 13, 1093487,
794 https://doi.org/10.3389/fmicb.2022.1093487, 2022.

795 Song, Y., Feng, H., Luo, S., Qi, J., Wang, X., Mei, W., Chen, N., Feng, Y., and Song, C.: Vertical
796 profiles of soil CO2 and CH4 emissions and their driving mechanisms in different types of permafrost
797 peatlands, J. Hydrol. (Amst)., 665, 134754, https://doi.org/10.1016/j.jhydrol.2025.134754, 2026.

798 Spiller, A., Kallenbach, C. M., Burnett, M. S., Olefeldt, D., Schulze, C., Maranger, R., and Douglas, P.
799 M. J.: Gradual drying of permafrost peat decreases carbon dioxide production in drier peat plateaus but
800 not in wetter fens and bogs, SOIL, 11, 371–379, https://doi.org/10.5194/soil-11-371-2025, 2025.

801 Strauss, J., Biasi, C., Sanders, T., Abbott, B. W., von Deimling, T. S., Voigt, C., Winkel, M.,
802 Marushchak, M. E., Kou, D., Fuchs, M., Horn, M. A., Jongejans, L. L., Liebner, S., Nitzbon, J.,
803 Schirrmeister, L., Walter Anthony, K., Yang, Y., Zubrzycki, S., Laboor, S., Treat, C., and Grosse, G.:
804 A globally relevant stock of soil nitrogen in the Yedoma permafrost domain, Nat. Commun., 13, 1–9,
805 https://doi.org/10.1038/s41467-022-33794-9, 2022.

806 Streletskiy, D. A., Nyland, K. E., Shiklomanov, N. I., Haggerty, E., Mann, M. L., Tolmanov, V., Nelson,
807 F. E., Klene, A. E., Pretis, F., Chen, L., Christiansen, H., de Pablo, M. A., Fyodorov-Davydov, D.,
808 Guglielmin, M., Hrbáček, F., Isaksen, K., Johansson, M., Leibman, M., Trombotto Liaudat, D.,
809 Maslakov, A., Mastepanov, M., Noetzli, J., Romanovsky, V. E., Sharkhuu, A., Smith, S. L., Abramov,
810 A., Babkina, E., Boike, J., Burn, C. R., Cannone, N., Cao, W., Davydov, S., Davydova, A., Delaloe, R.,
811 Douglas, T., Duchesne, C., Grebenets, V., Hauck, C., Hilbich, C., Hölzle, M., Kaufmann, R. K.,
812 Kholodov, A. L., Khomutov, A. V., Kňažkova, M., Konstantinov, P., Kuziakin, L., Lambiel, C., Li, G.,

https://doi.org/10.5194/egusphere-2026-5330
Preprint. Discussion started: 11 September 2026


Lupachev, A., Magnin, F., Sharkhuu, N., Orekhov, P., Pellet, C., Phillips, M., Pogliotti, P., Ponti, S., Rudd, D. A., Tregubov, O., Urban, F., Vieira, G., Vieli, A., Yu, W., Zamolodchikov, D., and Irrgang, A.: Long-term monitoring of active layer thickness confirms global permafrost degradation, Communications Earth & Environment 2026 7:1, 7, 671-, https://doi.org/10.1038/s43247-026-03824-1, 2026.

Swindles, G. T., Morris, P. J., Mullan, D., Watson, E. J., Turner, T. E., Roland, T. P., Amesbury, M. J., Kokfelt, U., Schoning, K., Pratte, S., Gallego-Sala, A., Charman, D. J., Sanderson, N., Garneau, M., Carrivick, J. L., Woulds, C., Holden, J., Parry, L., and Galloway, J. M.: The long-term fate of permafrost peatlands under rapid climate warming, Sci. Rep., 5, 17951, https://doi.org/10.1038/srep17951, 2015.

Szafranek-Nakonieczna, A. and Stêpniewska, Z.: Aerobic and anaerobic respiration in profiles of Polesie Lubelskie peatlands, Int. Agrophys., 28, 219–229, https://doi.org/10.2478/intag-2014-0011, 2014.

Tarkhov, M. O., Matyshak, G. V., Ryzhova, I. M., Goncharova, O. Y., Bobrik, A. A., Petrov, D. G., and Petrzhik, N. M.: Temperature Sensitivity of Soil Respiration in Palsa Peatlands of the North of Western Siberia, Eurasian Soil Science, 52, 945–953, https://doi.org/10.1134/S1064229319080155, 2019.

Treat, C. C., Wollheim, W. M., Varner, R. K., Grandy, A. S., Talbot, J., and Frolking, S.: Temperature and peat type control CO2 and CH4 production in Alaskan permafrost peats, Glob. Chang. Biol., 20, 2674–2686, https://doi.org/10.1111/gcb.12572, 2014.

Treat, C. C., Jones, M. C., Camill, P., Gallego-Sala, A., Garneau, M., Harden, J. W., Hugelius, G., Klein, E. S., Kokfelt, U., Kuhry, P., Loisel, J., Mathijssen, P. J. H., O'Donnell, J. A., Oksanen, P. O., Ronkainen, T. M., Sannel, A. B. K., Talbot, J., Tarnocai, C., and Väliranta, M.: Effects of permafrost aggradation on peat properties as determined from a pan-Arctic synthesis of plant macrofossils, J. Geophys. Res. Biogeosci., 121, 78–94, https://doi.org/10.1002/2015JG003061, 2016.

https://doi.org/10.5194/egusphere-2026-5330
Preprint. Discussion started: 11 September 2026


837 Vance, E. D., Brookes, P. C., and Jenkinson, D. S.: An extraction method for measuring soil microbial
838 biomass C, Soil Biol. Biochem., 19, 703–707, https://doi.org/10.1016/0038-0717(87)90052-6, 1987.

839 Voigt, C., Marushchak, M. E., Lamprecht, R. E., Jackowicz-Korczyński, M., Lindgren, A., Mastepanov,
840 M., Granlund, L., Christensen, T. R., Tahvanainen, T., Martikainen, P. J., and Biasi, C.: Increased
841 nitrous oxide emissions from Arctic peatlands after permafrost thaw, Proceedings of the National
842 Academy of Sciences, 114, 6238–6243, https://doi.org/10.1073/pnas.1702902114, 2017a.

843 Voigt, C., Lamprecht, R. E., Marushchak, M. E., Lind, S. E., Novakovskiy, A., Aurela, M., Martikainen,
844 P. J., and Biasi, C.: Warming of subarctic tundra increases emissions of all three important greenhouse
845 gases – carbon dioxide, methane, and nitrous oxide, Glob. Chang. Biol., 23, 3121–3138,
846 https://doi.org/10.1111/gcb.13563, 2017b.

847 Voigt, C., Marushchak, M. E., Mastepanov, M., Lamprecht, R. E., Christensen, T. R., Dorodnikov, M.,
848 Jackowicz-Korczyński, M., Lindgren, A., Lohila, A., Nykänen, H., Oinonen, M., Oksanen, T., Palonen,
849 V., Treat, C. C., Martikainen, P. J., and Biasi, C.: Ecosystem carbon response of an Arctic peatland to
850 simulated permafrost thaw, Glob. Chang. Biol., 25, 1746–1764, https://doi.org/10.1111/gcb.14574,
851 2019.

852 Voigt, C., Virkkala, A. M., Hould Gosselin, G., Bennett, K. A., Black, T. A., Detto, M., Chevrier-Dion,
853 C., Guggenberger, G., Hashmi, W., Kohl, L., Kou, D., Marquis, C., Marsh, P., Marushchak, M. E.,
854 Nesic, Z., Nykänen, H., Saarela, T., Sauheitl, L., Walker, B., Weiss, N., Wilcox, E. J., and Sonnentag,
855 O.: Arctic soil methane sink increases with drier conditions and higher ecosystem respiration, Nat. Clim.
856 Chang., 13, 1095–1104, https://doi.org/10.1038/s41558-023-01785-3, 2023.

857 Wang, Q., Zhao, X., Chen, L., Yang, Q., Chen, S., and Zhang, W.: Global synthesis of temperature
858 sensitivity of soil organic carbon decomposition: Latitudinal patterns and mechanisms, Funct. Ecol.,
859 33, 514–523, https://doi.org/10.1111/1365-2435.13256, 2019.

https://doi.org/10.5194/egusphere-2026-5330
Preprint. Discussion started: 11 September 2026


860 Wang, X., Song, C., Wang, J., Miao, Y., Mao, R., and Song, Y.: Carbon release from Sphagnum peat
861 during thawing in a montane area in China, Atmos. Environ., 75, 77–82,
862 https://doi.org/10.1016/j.atmosenv.2013.04.056, 2013.

863 Weishaar, J. L., Aiken, G. R., Bergamaschi, B. A., Fram, M. S., Fujii, R., and Mopper, K.: Evaluation
864 of specific ultraviolet absorbance as an indicator of the chemical composition and reactivity of dissolved
865 organic carbon, Environ. Sci. Technol., 37, 4702–4708, https://doi.org/10.1021/es030360x, 2003.

866 Wickham, H.: ggplot2: Elegant Graphics for Data Analysis, 2016., 2016.

867 Wickland, K. P., Waldrop, M. P., Aiken, G. R., Koch, J. C., Jorgenson, M. T., and Striegl, R. G.:
868 Dissolved organic carbon and nitrogen release from boreal Holocene permafrost and seasonally frozen
869 soils of Alaska, Environmental Research Letters, 13, 065011, https://doi.org/10.1088/1748-
870 9326/aac4ad, 2018.

871 Wild, B., Schnecker, J., Alves, R. J. E., Barsukov, P., Bárta, J., Čapek, P., Gentsch, N., Gittel, A.,
872 Guggenberger, G., Lashchinskiy, N., Mikutta, R., Rusalimova, O., Šantrůčková, H., Shibistova, O.,
873 Urich, T., Watzka, M., Zrazhevskaya, G., and Richter, A.: Input of easily available organic C and N
874 stimulates microbial decomposition of soil organic matter in arctic permafrost soil, Soil Biol. Biochem.,
875 75, 143–151, https://doi.org/10.1016/J.SOILBIO.2014.04.014, 2014.

876 Zhu, X., Burger, M., Doane, T. A., and Horwath, W. R.: Ammonia oxidation pathways and nitrifier
877 denitrification are significant sources of N2O and NO under low oxygen availability, Proc. Natl. Acad.
878 Sci. U. S. A., 110, 6328–6333, https://doi.org/10.1073/pnas.1219993110, 2013.

879 Zuo, Y., Song, Y., Jiang, L., Li, Y., Wang, Y., Chen, N., Jiang, P., Zheng, S., Song, C., Xu, X., Yuan,
880 F., and Sun, L.: Long-term carbon release of peatland soil after permafrost thaw in northmost China,
881 Catena (Amst)., 261, 109551, https://doi.org/10.1016/j.catena.2025.109551, 2025.

882
883

https://doi.org/10.5194/egusphere-2026-5330
Preprint. Discussion started: 11 September 2026


884 **13 Figures**

885

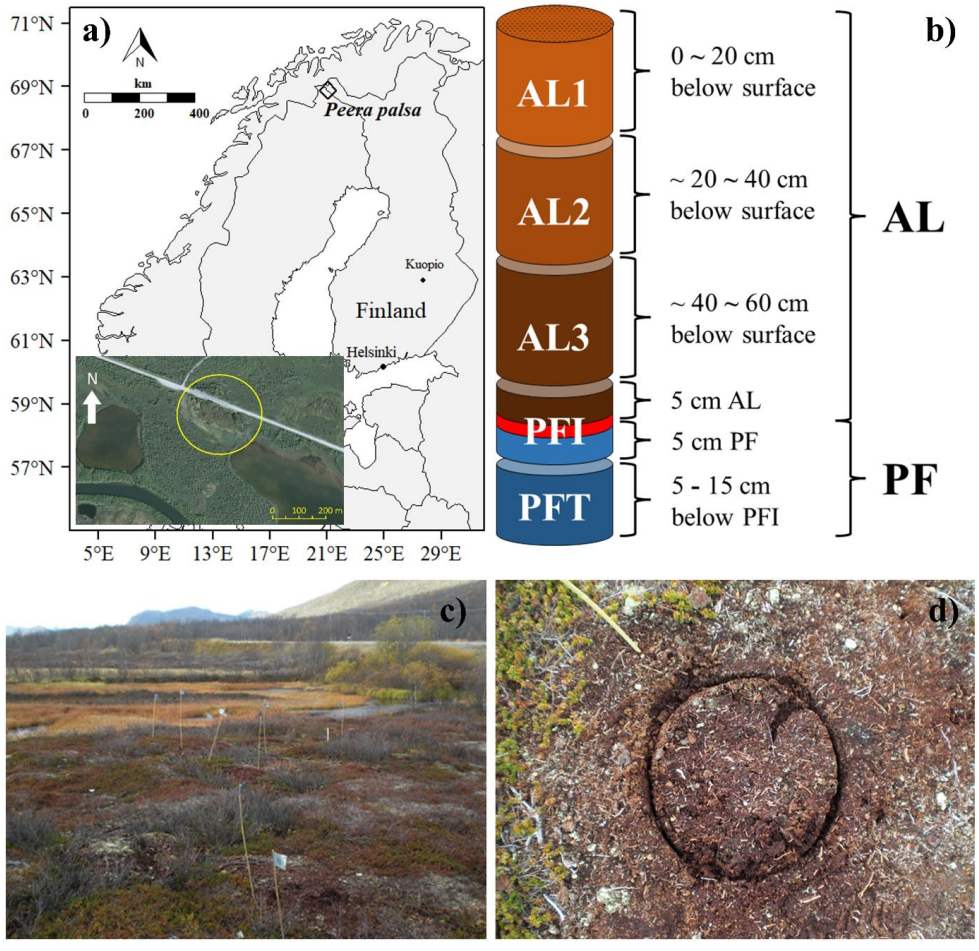


886

887 **Fig. 1: Intact peat soil core sampling site "Peera palsa". In a) the sampling site location in northern Finland and a**
888 **satellite image of the palsa complex (insert image source: © 2019 Google Maps, Airbus, CNES / Airbus, Lantmäteriet**
889 **/ Metria, Maxar Technologies). b) Scheme of the peat layer separation of the intact peat cores. The peat layer height of**
890 **the active layer fragments AL1, AL2 and AL3 varied by a few cm depending on the total depth of the active layer (see**
891 **supplementary information table S1). The permafrost interface layer (PFI) and the permafrost layer (PFT) had the**
892 **same height of 10 cm. The peat core diameter was 10 cm. c) Photograph of the palsa complex taken during the peat**
893 **core sampling. d) Photograph of a bare peat surface where the peat cores were sampled. Pictures were taken by C.**
894 **Voigt (2012).**

895

https://doi.org/10.5194/egusphere-2026-5330
Preprint. Discussion started: 11 September 2026


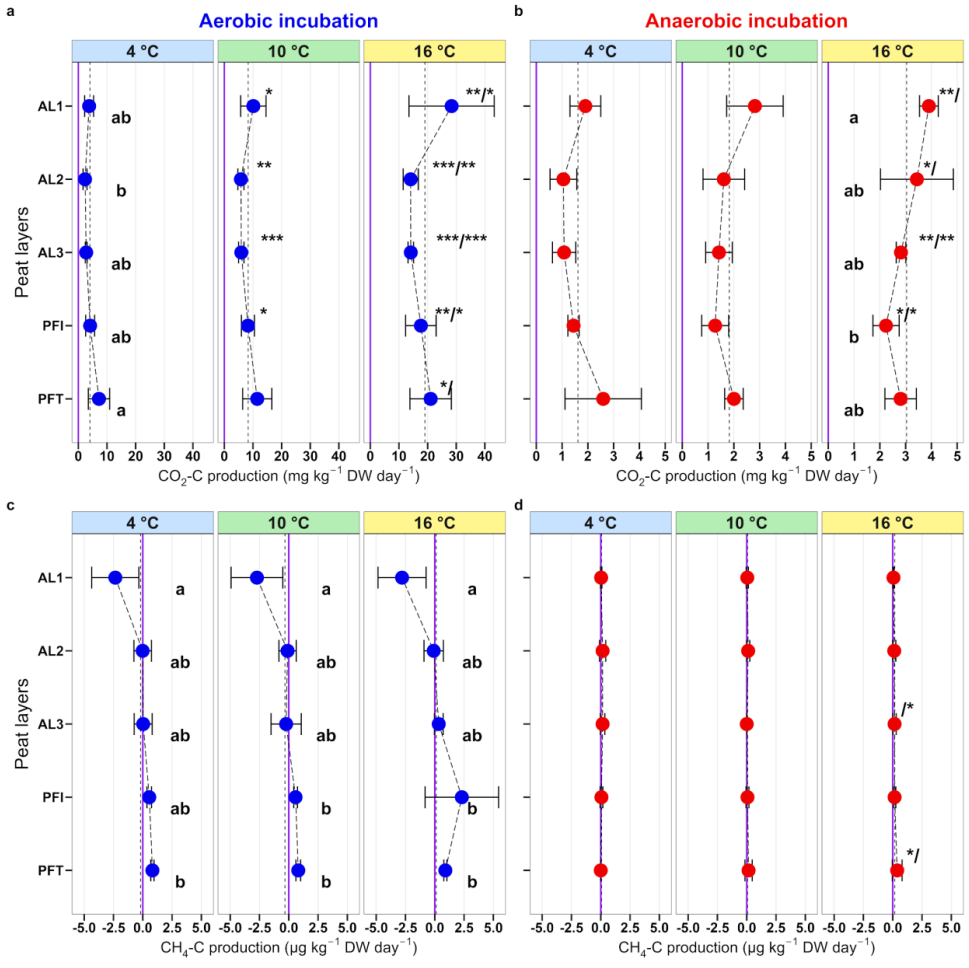


**Fig. 2: Daily aerobic (a) and anaerobic (b) CO2-C production rate (mg kg–1 DW (dry weight) day–1) and aerobic (c) and anaerobic (d) CH4-C production rate (µg kg–1 DW (dry weight) day–1) at 4, 10 and 16 °C during the incubation period of 161 days. Data points represent mean values; error bars show standard deviation (n = 4). Letters indicate statistical differences between peat layers within the given temperature (One-way ANOVA and Tukey's HSD, P ≤ 0.05). Asterisks indicate significant differences between incubation temperatures: for 10 °C, significant differences to 4 °C; for 16 °C significant difference to 4 °C/10 °C (One-way ANOVA). Dashed grey line in the background represents the mean value across all five peat layers at the given temperature. Level of significance: ***significant at P ≤ 0.001, ** significant at P ≤ 0.01, *significant at P ≤ 0.05. Note the different scales on X-axis for aerobic and anaerobic CO2-C production rate.**

https://doi.org/10.5194/egusphere-2026-5330
Preprint. Discussion started: 11 September 2026


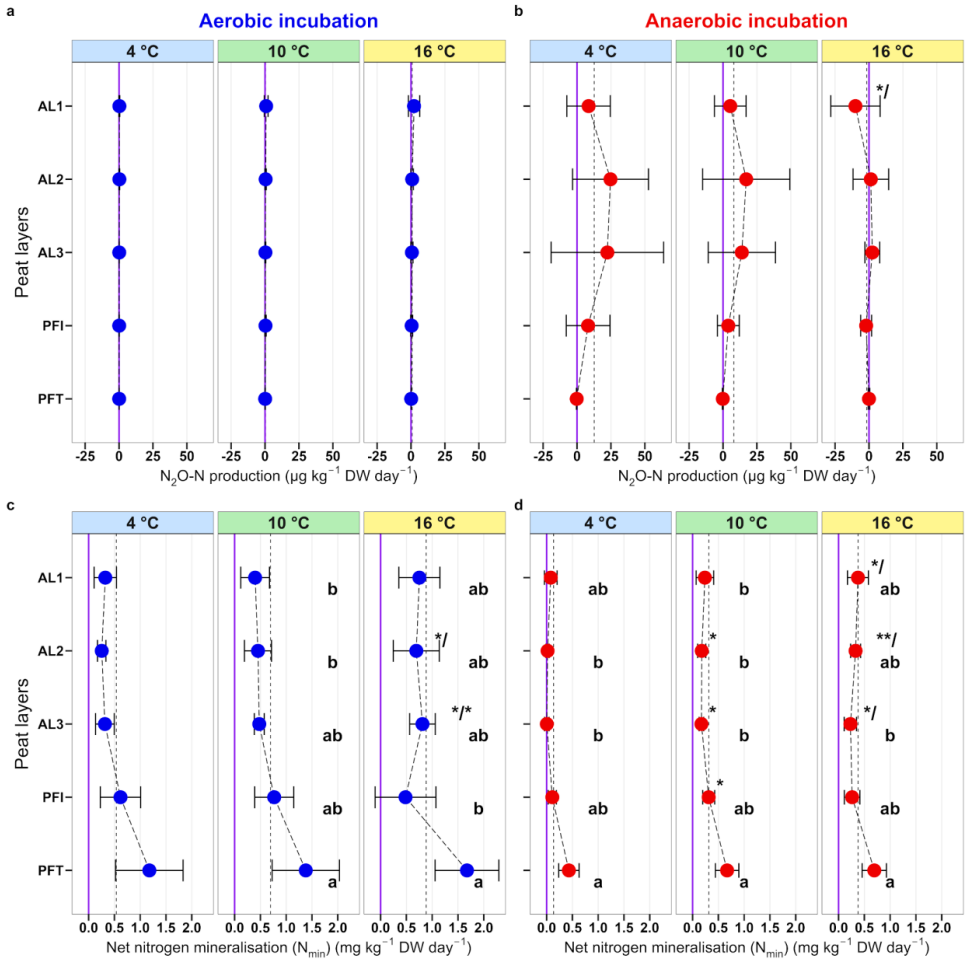


**Fig. 3: Daily aerobic (a) and anaerobic (b) N2O-N production rate (µg kg–1 DW (dry weight) day–1) and aerobic (c) and anaerobic (d) net nitrogen mineralization rate (mg kg–1 DW (dry weight) day–1) at 4, 10 and 16 °C during the incubation period of 161 days. Data points represent mean values; error bars show standard deviation (n = 4). Letters indicate statistical differences between peat layers within the given temperature (One-way ANOVA and Tukey's HSD, P ≤ 0.05). Asterisks indicate significant differences between incubation temperatures: for 10 °C, significant differences to 4 °C; for 16 °C significant difference to 4 °C/10 °C (One-way ANOVA). Dashed grey line in the background represents the mean value across all five peat layers at the given temperature. Level of significance: ***significant at P ≤ 0.001, ** significant at P ≤ 0.01, *significant at P ≤ 0.05.**

https://doi.org/10.5194/egusphere-2026-5330
Preprint. Discussion started: 11 September 2026


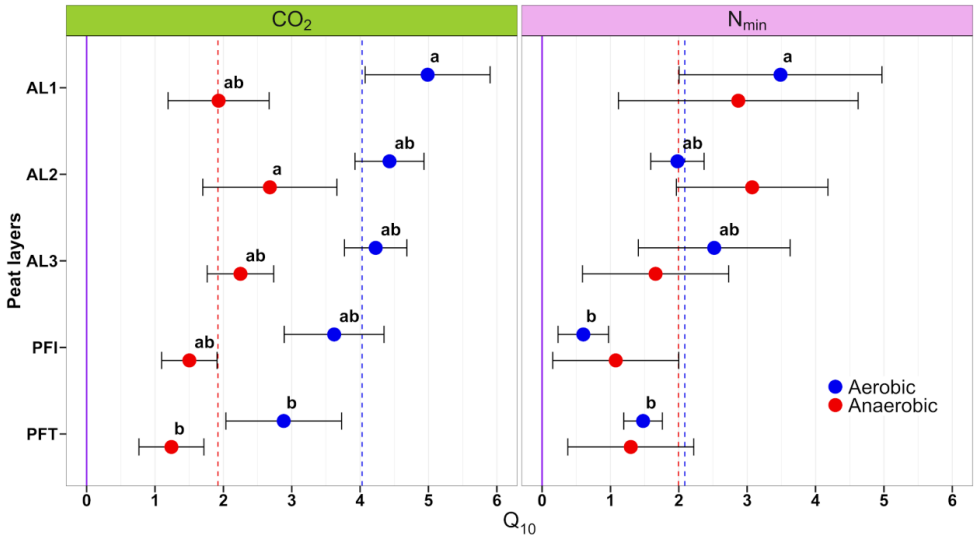


**Fig. 4: Temperature dependence of the five peat layers shown as Q10 values calculated for CO2-C production (CO2 - left panel) and net nitrogen mineralization (Nmin - right panel) in aerobic (blue) and anaerobic (red) incubation conditions. Data points represent mean values; error bars show standard deviation (n = 4). Letters indicate statistical differences (One-way ANOVA and Tukey's HSD, P ≤ 0.05) between the peat layers. Dashed coloured lines represent the mean Q10 values across all peat layers at aerobic and anaerobic incubation conditions.**

https://doi.org/10.5194/egusphere-2026-5330
Preprint. Discussion started: 11 September 2026


927

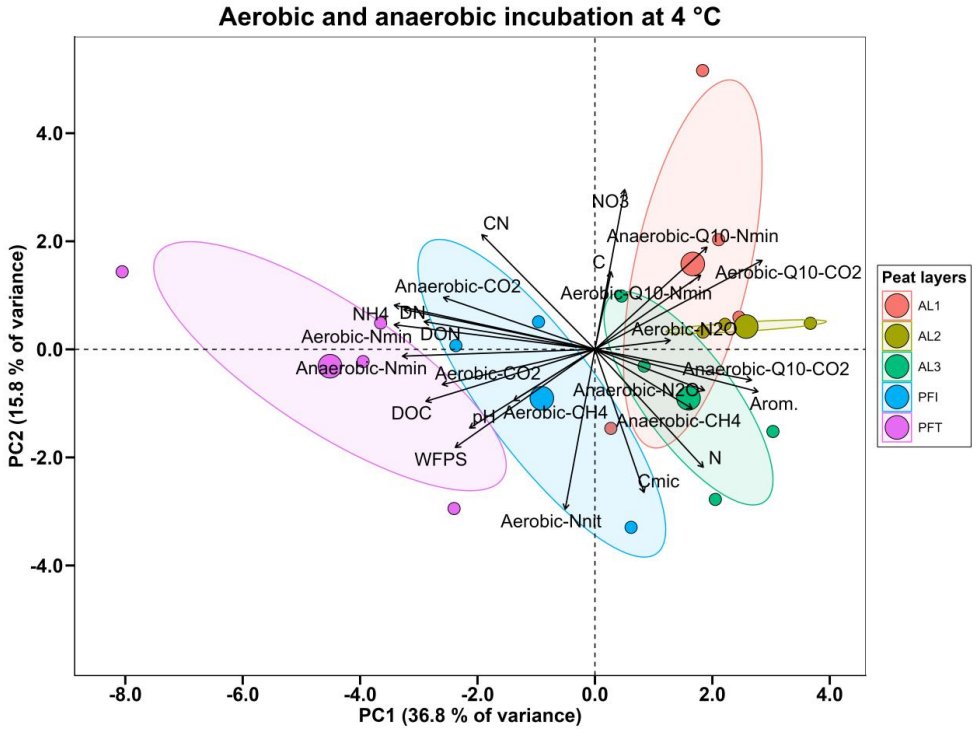


928

929 **Fig. 5: Principal component analysis (PCA) bi-plot of aerobic and anaerobic incubations at 4 °C. The analysed data**
930 **includes the cumulative GHG gas production over 161 incubation days; the temperature sensitivity of $CO_2$ production,**
931 **$Q_{10}CO_2$, and nitrogen mineralization, $Q_{10}N_{min}$; the net nitrogen mineralization rate ($N_{min}$) and net nitrification rate**
932 **($N_{nitr}$) (aerobic conditions only); in combination with soil chemical and physical parameters. Largest variability were**
933 **shown in the incubation temperature of 4 °C. Individual contributions of different variables to PC1 and PC2 are shown**
934 **in Figure S11.**

935

https://doi.org/10.5194/egusphere-2026-5330
Preprint. Discussion started: 11 September 2026


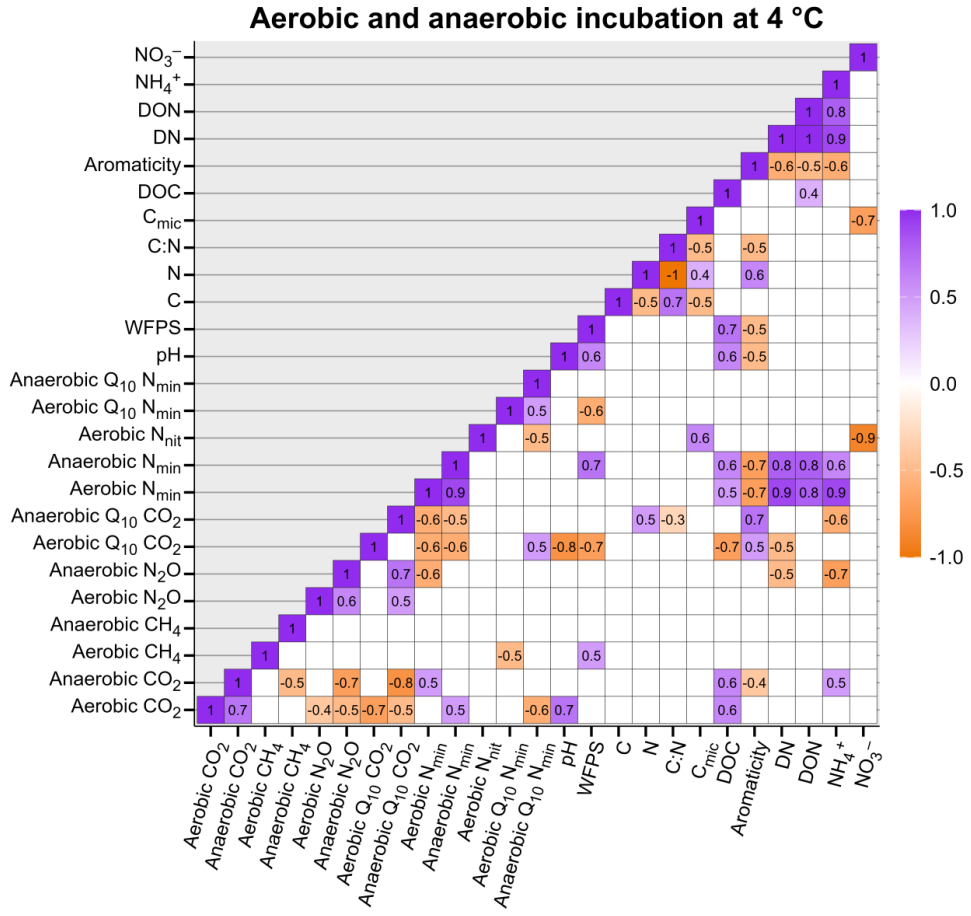


936

937 **Fig. 6: Pearson's correlation matrix of aerobic and anaerobic incubations at 4 °C. The analysed data includes the**
938 **cumulative GHG gas production over 161 incubation days; the temperature sensitivity of $CO_2$ production, $Q_{10}CO_2$ and**
939 **nitrogen mineralization, $Q_{10}N_{min}$; the net nitrogen mineralization rate ($N_{min}$) and net nitrification rate ($N_{nitr}$) (aerobic**
940 **conditions only); in combination with soil chemical and physical parameters.**

## 14 Tables

**Table 1: Peat characteristics of the peat layers analysed before the incubation experiment. Dry bulk density (BD), soil organic matter content (SOM - loss of ignition), water content ($H_2O$) water saturation from water holding capacity (WHC), water filled pore space (WFPS), total carbon (C) and total nitrogen (N) content, C:N ratio, pH, $K_2SO_4$ extractable dissolved organic carbon (DOC), total dissolved nitrogen (DN), dissolved organic nitrogen (DON), aromaticity of dissolved organic carbon, microbial biomass carbon (Cmic), $K_2SO_4$ extractable ammonium ($NH_4^+$) and $H_2O$ extractable nitrate ($NO_3$–). Values are mean ± standard deviation (n = 4). Different letters indicate statistical differences between the peat layers (One-way ANOVA and Tukey's HSD, $P \leq 0.05$).**

| Peat layer * | pH | BD (g $cm^{-3}$) | H2O (%) | WHC (%) | WFPS (%) | SOM (%) | C (%) | N (%) | C:N |
|---|---|---|---|---|---|---|---|---|---|
| AL1 | 3.7 ± 0.2 b | 0.16 ± 0.05 a | 68.8 ± 3.2 c | 46.6 ± 12.5 b | 40.7 ± 15.2 b | 99.94 ± 0.08 | 47.8 ± 5.0 | 1.3 ± 0.4 | 30.8 ± 8.3 |
| AL2 | 3.6 ± 0.1 b | 0.16 ± 0.03 ab | 72.0 ± 1.9 bc | 52.5 ± 6.6 b | 45.4 ± 9.7 b | 99.90 ± 0.10 | 47.2 ± 6.8 | 1.8 ± 0.3 | 27.5 ± 6.8 |
| AL3 | 3.9 ± 0.3 ab | 0.12 ± 0.03 ab | 76.5 ± 3.2 b | 49.2 ± 7.5 b | 43.7 ± 8.3 b | 99.91 ± 0.10 | 47.1 ± 6.6 | 1.7 ± 0.2 | 29.4 ± 7.6 |
| PFI | 4.2 ± 0.5 ab | 0.10 ± 0.01 ab | 83.9 ± 2.2 a | 57.4 ± 8.9 ab | 58.5 ± 9.9 ab | 99.91 ± 0.07 | 47.5 ± 4.4 | 1.5 ± 0.4 | 33.3 ± 9.7 |
| PFT | 4.7 ± 0.7 a | 0.09 ± 0.01 b | 88.9 ± 1.7 a | 73.3 ± 8.1 a | 76.9 ± 6.9 a | 99.92 ± 0.04 | 47.7 ± 1.7 | 1.4 ± 0.4 | 37.5 ± 11.9 |
| Average | 4.0 ± 0.6 | 0.13 ± 0.04 | 78.0 ± 8.0 | 55.8 ± 12.6 | 53.1 ± 16.5 | 99.92 ± 0.07 | 47.4 ± 4.7 | 1.6 ± 0.3 | 31.7 ± 8.8 |

| Peat layer * | $C_{mic}$ (mg C $kg_{-1}$ DW) | DOC (mg C $kg_{-1}$ DW) | Aromaticity (% DOC) | DN (mg N $kg_{-1}$ DW) | DON (mg N $kg_{-1}$ DW) | $NH_4^+$ (mg N $kg_{-1}$ DW) | $NO_3^-$ (mg N $kg_{-1}$ DW) |
|---|---|---|---|---|---|---|---|
| AL1 | 710.8 ± 295.4 | 854.9 ± 186.7 b | 28.9 ± 9.6 a | 166.2 ± 94.5 | 131.0 ± 82.8 | 29.8 ± 16.9 | 5.4 ± 5.1 |
| AL2 | 847.6 ± 243.8 | 964.4 ± 322.7 ab | 32.8 ± 2.7 a | 117.9 ± 55.5 | 100.7 ± 57.5 | 14.2 ± 5.2 | 3.4 ± 2.7 |
| AL3 | 1337.4 ± 1022.9 | 838.3 ± 142.9 b | 24.7 ± 4.4 ab | 140.8 ± 77.3 | 111.2 ± 58.8 | 28.1 ± 19.2 | 1.5 ± 1.5 |
| PFI | 1275.8 ± 707.6 | 915.3 ± 133.1 ab | 20.8 ± 4.1 ab | 177.7 ± 81.3 | 103.1 ± 31.0 | 73.6 ± 50.0 | 0.9 ± 0.8 |
| PFT | 880.9 ± 305.2 | 1525.4 ± 481.9 a | 12.9 ± 4.2 b | 359.1 ± 199.3 | 233.1 ± 107.1 | 123.3 ± 95.7 | 2.6 ± 3.2 |
| Average | 1010.5 ± 589.5 | 1019.7 ± 366.1 | 24.0 ± 8.6 | 192.3 ± 133.9 | 135.8 ± 82.0 | 53.8 ± 60.3 | 2.7 ± 3.1 |

* Active layer 1, 2, 3 (AL1, 2, 3), permafrost interface (PFI), permafrost table (PFT) (see Fig. 1b)

https://doi.org/10.5194/egusphere-2026-5330
Preprint. Discussion started: 11 September 2026


**Table 2: Aerobic and anaerobic incubation differences: linear mixed effects model estimates of fixed effects, SE, t-value, lower and upper confidence intervals and P-values for cumulative production of $CO_2$, $CH_4$ and $N_2O$, net N mineralization ($N_{min}$) rates and the $Q_{10}$ of $CO_2$ production and net N mineralization.**

| Fixed effects | Estimate | SE | *t*-value | 2.5% CI | 97.5% CI | *P*-value | Significance |
|---|---|---|---|---|---|---|---|
| $CO_2$ production | | | | | | | |
| (Intercept) | 3.099 | 0.054 | 57.552 | 2.992 | 3.206 | <0.001 | *** |
| Oxic condition: Anaerobic | -0.614 | 0.052 | -11.795 | -0.717 | -0.511 | <0.001 | *** |
| $CH_4$ production | | | | | | | |
| (Intercept) | -0.037 | 0.019 | -1.914 | -0.075 | 0.001 | 0.058 | |
| Oxic condition: Anaerobic | 0.044 | 0.023 | 1.959 | -0.001 | 0.089 | 0.053 | |
| $N_2O$ production | | | | | | | |
| (Intercept) | 0.076 | 0.358 | 0.213 | -0.632 | 0.785 | 0.832 | |
| Oxic condition: Anaerobic | 0.948 | 0.389 | 2.433 | 0.176 | 1.719 | 0.017 | * |
| Net N mineralization ($N_{min}$) | | | | | | | |
| (Intercept) | 0.213 | 0.022 | 9.559 | 0.169 | 0.257 | <0.001 | *** |
| Oxic condition: Anaerobic | -0.113 | 0.018 | -6.168 | -0.149 | -0.076 | <0.001 | *** |
| $Q_{10}$ $CO_2$ production ($Q_{10}CO_2$) | | | | | | | |
| (Intercept) | 4.029 | 0.154 | 26.107 | 3.723 | 4.334 | <0.001 | *** |
| Oxic condition: Anaerobic | -2.108 | 0.155 | -13.599 | -2.415 | -1.801 | <0.001 | *** |
| $Q_{10}$ net N mineralization ($Q_{10}N_{min}$) | | | | | | | |
| (Intercept) | 2.091 | 0.213 | 9.836 | 1.670 | 2.513 | <0.001 | *** |
| Oxic condition: Anaerobic | -0.096 | 0.233 | -0.411 | -0.557 | 0.366 | 0.682 | |

Level of significance: * $p < 0.05$, ** $p < 0.01$, *** $p < 0.001$

https://doi.org/10.5194/egusphere-2026-5330
Preprint. Discussion started: 11 September 2026


952 **Table 3: Linear mixed effects model estimates of fixed effects, SE, t-value, lower and upper confidence intervals and P-**
953 **values of aerobic and anaerobic cumulative production of $CO_2$, $CH_4$ and the $Q_{10}$ of $CO_2$ production.**

| Fixed effects | Estimate | SE | *t*-value | 2.5% CI | 97.5% CI | *P*-value | Significance |
|---|---|---|---|---|---|---|---|
| Aerobic $CO_2$ production | | | | | | | |
| (Intercept) | 2.835 | 0.071 | 39.853 | 2.692 | 2.978 | <0.001 | *** |
| Incubation temperature: 10 °C | 0.338 | 0.037 | 9.205 | 0.264 | 0.411 | <0.001 | *** |
| Incubation temperature: 16 °C | 0.701 | 0.037 | 19.103 | 0.627 | 0.775 | <0.001 | *** |
| Peat layer: AL2 | -0.223 | 0.047 | -4.716 | -0.319 | -0.128 | <0.001 | *** |
| Peat layer: AL3 | -0.190 | 0.047 | -4.001 | -0.285 | -0.094 | <0.001 | *** |
| Peat layer: PFI | -0.067 | 0.047 | -1.405 | -0.162 | 0.029 | 0.166 | |
| Peat layer: PFT | 0.066 | 0.047 | 1.394 | -0.029 | 0.161 | 0.169 | |
| Anaerobic $CO_2$ production | | | | | | | |
| (Intercept) | 2.503 | 0.061 | 40.998 | 2.381 | 2.626 | <0.001 | *** |
| Incubation temperature: 10 °C | 0.066 | 0.051 | 1.294 | -0.036 | 0.168 | 0.202 | |
| Incubation temperature: 16 °C | 0.313 | 0.051 | 6.168 | 0.211 | 0.415 | <0.001 | *** |
| Peat layer: AL2 | -0.208 | 0.066 | -3.171 | -0.340 | -0.076 | 0.003 | ** |
| Peat layer: AL3 | -0.227 | 0.066 | -3.468 | -0.359 | -0.096 | 0.001 | ** |
| Peat layer: PFI | -0.231 | 0.066 | -3.518 | -0.362 | -0.099 | <0.001 | *** |
| Peat layer: PFT | -0.055 | 0.066 | -0.840 | -0.187 | 0.077 | 0.405 | |
| Aerobic $CH_4$ production | | | | | | | |
| (Intercept) | -0.292 | 0.047 | -6.252 | -0.386 | -0.198 | <0.001 | *** |
| Incubation temperature: 10 °C | -0.021 | 0.035 | -0.600 | -0.092 | 0.049 | 0.551 | |
| Incubation temperature: 16 °C | 0.009 | 0.035 | 0.267 | -0.061 | 0.080 | 0.791 | |
| Peat layer: AL2 | 0.288 | 0.045 | 6.360 | 0.197 | 0.379 | <0.001 | *** |
| Peat layer: AL3 | 0.295 | 0.045 | 6.513 | 0.204 | 0.386 | <0.001 | *** |
| Peat layer: PFI | 0.361 | 0.045 | 7.961 | 0.270 | 0.452 | <0.001 | *** |
| Peat layer: PFT | 0.351 | 0.045 | 7.754 | 0.260 | 0.442 | <0.001 | *** |
| Anaerobic $CH_4$ production | | | | | | | |
| (Intercept) | 0.001 | 0.004 | 0.296 | -0.007 | 0.009 | 0.768 | |
| Incubation temperature: 10 °C | 0.000 | 0.004 | -0.082 | -0.008 | 0.007 | 0.935 | |
| Incubation temperature: 16 °C | 0.006 | 0.004 | 1.705 | -0.001 | 0.014 | 0.094 | |
| Peat layer: AL2 | 0.006 | 0.005 | 1.211 | -0.004 | 0.016 | 0.232 | |
| Peat layer: AL3 | 0.004 | 0.005 | 0.782 | -0.006 | 0.014 | 0.438 | |
| Peat layer: PFI | 0.003 | 0.005 | 0.634 | -0.007 | 0.013 | 0.529 | |
| Peat layer: PFT | 0.009 | 0.005 | 1.751 | -0.001 | 0.018 | 0.086 | |
| Aerobic $Q_{10}$ $CO_2$ production | | | | | | | |
| (Intercept) | 4.986 | 0.258 | 19.312 | 4.468 | 5.504 | <0.001 | *** |
| Peat layer: AL2 | -0.559 | 0.213 | -2.627 | -0.987 | -0.132 | 0.011 | * |
| Peat layer: AL3 | -0.756 | 0.213 | -3.551 | -1.183 | -0.329 | <0.001 | *** |
| Peat layer: PFI | -1.367 | 0.213 | -6.418 | -1.794 | -0.939 | <0.001 | *** |
| Peat layer: PFT | -2.105 | 0.213 | -9.886 | -2.532 | -1.678 | <0.001 | *** |
| Anaerobic $Q_{10}$ $CO_2$ production | | | | | | | |
| (Intercept) | 1.932 | 0.189 | 10.237 | 1.553 | 2.310 | <0.001 | *** |
| Peat layer: AL2 | 0.750 | 0.232 | 3.236 | 0.285 | 1.214 | 0.002 | ** |
| Peat layer: AL3 | 0.319 | 0.232 | 1.375 | -0.146 | 0.783 | 0.175 | |
| Peat layer: PFI | -0.43 | 0.232 | -1.856 | -0.895 | 0.035 | 0.069 | |
| Peat layer: PFT | -0.693 | 0.232 | -2.991 | -1.157 | -0.228 | 0.004 | ** |

Level of significance: * $p < 0.05$, ** $p < 0.01$, *** $p < 0.001$

954

https://doi.org/10.5194/egusphere-2026-5330
Preprint. Discussion started: 11 September 2026


**Table 4: Linear mixed effects model estimates of fixed effects, SE, t-value, lower and upper confidence intervals and P-values of aerobic and anaerobic cumulative production of $N_2O$, the net N mineralization and net nitrification rates and the $Q_{10}$ of net N mineralization.**

| Fixed effects | Estimate | SE | *t*-value | 2.5% CI | 97.5% CI | *P*-value | Significance |
|---|---|---|---|---|---|---|---|
| Aerobic $N_2O$ production | | | | | | | |
| (Intercept) | 0.127 | 0.066 | 1.916 | -0.006 | 0.259 | 0.061 | |
| Incubation temperature: 10 °C | 0.038 | 0.057 | 0.668 | -0.076 | 0.153 | 0.507 | |
| Incubation temperature: 16 °C | 0.113 | 0.057 | 1.977 | -0.002 | 0.227 | 0.053 | |
| Peat layer: AL2 | -0.095 | 0.074 | -1.286 | -0.242 | 0.053 | 0.204 | |
| Peat layer: AL3 | -0.120 | 0.074 | -1.625 | -0.267 | 0.028 | 0.110 | |
| Peat layer: PFI | -0.128 | 0.074 | -1.743 | -0.276 | 0.019 | 0.087 | |
| Peat layer: PFT | -0.161 | 0.074 | -2.183 | -0.308 | -0.013 | 0.034 | * |
| Anaerobic $N_2O$ production | | | | | | | |
| (Intercept) | 1.234 | 1.049 | 1.176 | -0.872 | 3.339 | 0.245 | |
| Incubation temperature: 10 °C | -0.754 | 0.871 | -0.865 | -2.503 | 0.995 | 0.391 | |
| Incubation temperature: 16 °C | -2.313 | 0.871 | -2.655 | -4.062 | -0.564 | 0.011 | * |
| Peat layer: AL2 | 2.104 | 1.125 | 1.870 | -0.154 | 4.361 | 0.067 | |
| Peat layer: AL3 | 1.865 | 1.125 | 1.658 | -0.393 | 4.123 | 0.103 | |
| Peat layer: PFI | 0.324 | 1.125 | 0.288 | -1.934 | 2.582 | 0.774 | |
| Peat layer: PFT | -0.232 | 1.125 | -0.206 | -2.490 | 2.026 | 0.838 | |
| Aerobic net N mineralization ($N_{min}$) | | | | | | | |
| (Intercept) | 0.121 | 0.04 | 3.043 | 0.041 | 0.201 | 0.004 | ** |
| Incubation temperature: 10 °C | 0.044 | 0.026 | 1.684 | -0.008 | 0.096 | 0.098 | |
| Incubation temperature: 16 °C | 0.084 | 0.026 | 3.236 | 0.032 | 0.137 | 0.002 | ** |
| Peat layer: AL2 | -0.006 | 0.034 | -0.186 | -0.074 | 0.061 | 0.853 | |
| Peat layer: AL3 | 0.016 | 0.034 | 0.475 | -0.052 | 0.084 | 0.637 | |
| Peat layer: PFI | 0.031 | 0.034 | 0.913 | -0.037 | 0.098 | 0.366 | |
| Peat layer: PFT | 0.203 | 0.034 | 6.026 | 0.135 | 0.271 | <0.001 | *** |
| Anaerobic net N mineralization ($N_{min}$) | | | | | | | |
| (Intercept) | 0.036 | 0.017 | 2.084 | 0.001 | 0.071 | 0.042 | * |
| Incubation temperature: 10 °C | 0.063 | 0.012 | 5.207 | 0.039 | 0.088 | <0.001 | *** |
| Incubation temperature: 16 °C | 0.084 | 0.012 | 6.949 | 0.06 | 0.109 | <0.001 | *** |
| Peat layer: AL2 | -0.015 | 0.016 | -0.954 | -0.047 | 0.017 | 0.345 | |
| Peat layer: AL3 | -0.033 | 0.015 | -2.134 | -0.064 | -0.002 | 0.038 | * |
| Peat layer: PFI | 0.001 | 0.015 | 0.077 | -0.03 | 0.032 | 0.939 | |
| Peat layer: PFT | 0.113 | 0.015 | 7.343 | 0.082 | 0.144 | <0.001 | *** |
| Aerobic net nitrification ($N_{nit}$) | | | | | | | |
| (Intercept) | -1.198 | 0.09 | -13.254 | -1.379 | -1.017 | <0.001 | *** |
| Incubation temperature: 10 °C | 0.278 | 0.082 | 3.409 | 0.114 | 0.442 | 0.001 | ** |
| Incubation temperature: 16 °C | 0.159 | 0.082 | 1.953 | -0.004 | 0.323 | 0.056 | |
| Peat layer: AL2 | 0.161 | 0.105 | 1.531 | -0.05 | 0.373 | 0.132 | |
| Peat layer: AL3 | 0.141 | 0.105 | 1.34 | -0.07 | 0.353 | 0.186 | |
| Peat layer: PFI | 0.174 | 0.105 | 1.654 | -0.037 | 0.386 | 0.104 | |
| Peat layer: PFT | 0.025 | 0.105 | 0.24 | -0.186 | 0.237 | 0.812 | |

Level of significance: * $p < 0.05$, ** $p < 0.01$, *** $p < 0.001$

https://doi.org/10.5194/egusphere-2026-5330
Preprint. Discussion started: 11 September 2026


**Table 4: continued**

| | | | | | | | |
|---|---|---|---|---|---|---|---|
| Aerobic $Q_{10}$ net N mineralization | | | | | | | |
| (Intercept) | 3.486 | 0.240 | 14.538 | 3.005 | 3.968 | <0.001 | *** |
| Peat layer: AL2 | -1.506 | 0.325 | -4.627 | -2.160 | -0.852 | <0.001 | *** |
| Peat layer: AL3 | -0.969 | 0.325 | -2.978 | -1.623 | -0.315 | 0.004 | ** |
| Peat layer: PFI | -2.870 | 0.353 | -8.128 | -3.579 | -2.161 | <0.001 | *** |
| Peat layer: PFT | -2.010 | 0.325 | -6.175 | -2.663 | -1.356 | <0.001 | *** |
| Anaerobic $Q_{10}$ net N mineralization | | | | | | | |
| (Intercept) | 2.868 | 0.408 | 7.028 | 2.049 | 3.686 | <0.001 | *** |
| Peat layer: AL2 | 0.204 | 0.377 | 0.540 | -0.553 | 0.960 | 0.592 | |
| Peat layer: AL3 | -1.206 | 0.377 | -3.196 | -1.962 | -0.449 | 0.002 | ** |
| Peat layer: PFI | -1.789 | 0.377 | -4.743 | -2.546 | -1.033 | <0.001 | *** |
| Peat layer: PFT | -1.570 | 0.377 | -4.162 | -2.327 | -0.814 | <0.001 | *** |

Level of significance: * $p < 0.05$, ** $p < 0.01$, *** $p < 0.001$